Modelling stream flow with a discrete rainfall-runoff model and 37GHz PDBT microwave observations: the Xiangjiang River basin case study

Haolu Shang[1,2], Massimo Menenti[2,1], Li Jia[1]

[1]Stake Key Laboratory of Remote Sensing Science, Institute of Remote Sensing and Digital Earth, Chinese Academy of Sciences. Beijing 100101, China
[2]Geoscience and Remote Sensing, Delft University of Technology, Delft, 2628 CN Delft / 2600 GA Delft, The Netherlands

Correspondence to: Li Jia (jiali@radi.ac.cn)

Abstract. A discrete rainfall-runoff model was developed, which can fully use the fractional area of Water Saturated Soil (WSS) and inundation area retrieved from 37 GHz microwave observations to calculate overland and infiltrated flows. The model assumes that specific runoff integrates the contributions of precipitation over a certain period. This duration determines the number of model parameters and can vary from weeks to months. The model was implemented at three levels of increasing complexity with precipitation, ground water table depth, and the WSS and inundated area, which are designed to reduce the duration required to achieve a reasonable performance. The three levels are defined by the key-variables as: 1) precipitation and base flow; 2) overland flow, infiltrated flow and base flow; 3) overland flow, potential subsurface flow and base flow. The set of model parameters driving each implementation is easy to calibrate with a linear regression method, and is an indication of dominant hydrological processes, particularly water storage, in determining the catchment response to rainfall. The three model implementations were calibrated with the 10-day averaged river discharge in 2002 (wet) and 2005 (dry) at Changsha station, downstream of Xiangjiang River basin, China. The second and third implementations had better performance than the first one in both years when the duration was increased step-wisely from 10 days to 100 days , with $0.78 \leq$Nash-Sutcliffe Efficiency (NSE) ≤ 0.97 and $12\% \leq$ Relative Root Mean Square Error (RRMSE)$\leq 34\%$. Cross validation results showed that when the duration ≤ 100 days, the model improvement from the first to the second and third implementations was due to the application of the WSS and inundated area. All model implementations were evaluated against observed discharges in 2001. The second and third implementations performed better than the first one, with NSE $\approx$0.83 and RRMSE $\approx$ 34%, when using model parameters averaged over 2002 and 2005 and the durations of antecedent precipitation of 10. The first implementation needed much longer duration of antecedent precipitation to achieve a similar performance. The calibration and validation process proves that the retrievals of WSS and inundated area can reduce the required duration of antecedent precipitation, i.e. to achieve a satisfactory performance with fewer model parameters, and justifies the method to estimate the potential subsurface flow. The RRMSE of each season at the calibration stage indicates the possible ground water recharge period, i.e. 90 days, in the Xiangjiang River basin. The complexity as the second

implementation was enough to achieve a stable prediction of stream flows in different years, using the parameters averaged over dry and wet years and the duration of 10 days.

Keywords: Passive microwave, Water Saturated Soil, Discrete rainfall-runoff model, Regional water storage.

1 Introduction

In many conceptual hydrological models, such as the Xinganjiang model (Zhao, 1977, 1984), Probability Distributed Model (PDM) (Moore, 2007, 1985), TOPMODEL (Beven and Kirkby, 1979; Beven et al., 1984), Variable Infiltration Capacity (VIC) model (Liang et al., 1994; Wood et al., 1992) and ARNO (Todini, 1996) , water saturated soil is a conceptual parameter that determines the fast runoff produced after a storm, i.e. overland flow and fast subsurface flow. Fractional area of water saturated soil can be derived from regional water storage with some physically parameters, such as the topography-soil index in TOPMODEL (Sivapalan et al., 1987) or the infiltration factor in VIC (Liang et al., 1994; Wood et al., 1992). It is, however, difficult to measure regional water storage precisely (Eagleson, 1978) and to optimise these physical parameters for various catchments. In our previous study, we have shown that the fractional area of Water Saturated Soil (WSS) and inundated area can be retrieved from the Polarization Difference Brightness Temperature (PDBT) observed by space-borne microwave radiometers at 37 GHz, after taking the influence of the vegetation and the atmosphere into account. The WSS and inundated area is where open water or water-saturated top soil occurs, such as wet lands, ponds, lakes and rivers, and it is a potentially useful input to these conceptual hydrological models towards mitigation of data requirements and simpler model calibration.

The difference between the WSS and inundated area and the conceptual water saturated soil is significant. The WSS and inundated area only represents the water saturation in the top soil, while the depth of the water saturated soil in a conceptual model is variable, depending on water storage, soil porosity and the topography (Beven and Kirkby, 1979; Wood et al., 1992). A possible method to bridge this difference is to assimilate regional soil moisture using a soil-canopy-atmosphere model and the observations from Special Sensor Microwave Imager (SSM/I) as shown by Lakshmi et al. (1997a, 1997b). In their study, microwave observations at lower frequencies (e.g. 19 GHz), however, were preferred, rather than at 37 GHz, because the penetration depth at 37 GHz is too shallow (i.e. 0.08cm – 0.8 cm). The parameterization of the soil-canopy-atmosphere model adds to the difficulty and uncertainty in this assimilation method (see e.g. Lakshmi et al. (1997a)). Hydrological models provide reasonably accurate estimates of soil water content, while model estimates of spatial patterns, like the delineation of inundated areas and wetlands, are rather challenging, because of the required spatially detailed data on soil texture, soil porosity, vegetation and ground water table depth, as documented by the studies on wetlands in the prairies of North America (Hayashi et al., 1998; Kazezyılmaz-Alhan et al., 2007; Shjeflo, 1968; Su et al., 2000; Winter and Rosenberry, 1995; Winter and Valk, 1989; Woo and Rowsell, 1993). On the other hand, many studies showed a straightforward but lagged relationship between the WSS and inundated area and the river discharge or stage. In our previous

study (Shang et al., 2015), the upstream WSS and inundated areas were highly correlated with the Poyang Lake area downstream, with a time lag between 3 and 5 days. This finding suggests that the inundated area retrieved from microwave observation at 37 GHz might be used directly to estimate river discharge or stage with a certain rating curve and a modification on time lags (Sippel et al., 1998; Temimi et al., 2005; Vörösmarty et al., 1996). These results suggest also that conceptual hydrological models might be simplified significantly by using retrievals of the WSS and inundated area.

The WSS and inundated area is the result of comprehensive processes at surface including precipitation, evapotranspiration, regional water storage and drainage. It determines the partition of precipitation into overland and infiltrated flows (Beven and Kirkby, 1979; Liang et al., 1994; Sivapalan et al., 1987; Wood et al., 1992). One advantage of the retrievals of the WSS and inundated area with PDBT at 37 GHz is that it provides daily observation. To fully use such high frequency observations of surface wetness conditions, we developed a lumped hydrological model, i.e. the discrete rainfall-runoff model, based on the redistribution of antecedent precipitation. Many hydrological processes result in this redistribution. For example, in a storm event, a fraction of precipitation produces fast flow, i.e. over land flow and fast subsurface flow, while the remaining precipitation is stored in subsurface and ground water and produces subsurface and base flow, during a recession period (Beven and Kirkby, 1979; Moore, 1985; Sivapalan et al., 1987; Sophocleous, 2002; Todini, 1996; Wood et al., 1992; Xu and Singh, 2004). Antecedent precipitation reaches rivers and channels at different times. During the period when overland flow is drained by channels and rivers, a fraction of overland flow may percolate into the subsurface, be stored into lakes, wetlands and reservoirs, or be used by human activities (e.g. irrigation). The stored or consumed overland flow will be released to stream flow with a time lag (see e.g. Vörösmarty et al. (1996)). The water stored in soil and ground water interacts with surface water and stream flow through complicated processes in a dynamic way (see e.g. Mertes (1997); Sophocleous (2002)). These processes redistribute antecedent precipitation within a catchment into its components over different periods of time, which results in the time lag between precipitation and stream flow (Gleick, 1987). The lagged release of overland flow and the interactions between surface and soil layers complicate the redistribution of precipitation in time.

In VIC model, precipitation is partitioned into direct runoff (e.g. overland flow and fast subsurface flow) and slow runoff released from soil layers, according to the regional water storage and the infiltration capacity parameter (Wood et al., 1992). Jakeman and Hornberger (1993); Jakeman et al. (1990) developed the two component linear model, i.e. quick and slow flows, to simulate the time series of stream flow from the precipitation time series, according to their statistical relationship. These physical or statistical approaches clearly show that precipitation contributes to stream flow at different time lags. The VIC model can take the interaction between water flows and various water storages into account by estimating the regional water storage from satellite observations (e.g. Lakshmi et al. (1997a)), while the two component linear model did not take that into account. Our discrete rainfall-runoff model combines the physical basis of the VIC model with the relationship between the time series of stream flow and precipitation, so that to reduce the complication in the calibration for the conceptual models. Our model assumes that stream flow integrates the contributions of precipitation or specific component flows within a certain period. The weight of each contribution to stream flow at a given time constitutes the core of our model and depends

on the duration of antecedent precipitation. This duration can vary from days to months. Long duration means a large number of model parameters, which may lead to the problem of overfitting. Thus a relatively short duration is preferred in the model implementation.

Observed ground water table depth and the retrieved WSS and inundated area are used to develop three implementations of the discrete rainfall-runoff model with increasing complexity. We want to evaluate whether the increasing complexity in the model implementations can reduce the duration of antecedent precipitation required to achieve a reasonable performance. One advantage of the three implementations is that they can be calibrated with a linear regression method, much easier than the calibration methods used by other conceptual hydrological models, e.g. automatic calibration (Gupta et al., 1999; Madsen, 2000). This linear regression method may lead to the problem of overfitting, i.e. the model reproduces the calibration data set just because of the number of model parameters being comparable with the number of observations (Babyak, 2004; Hawkins, 2004). .

Another advantage of using the retrieved WSS and inundated area is fewer data are required for calibration, compared with other conceptual models, since some complicated hydrological processes, e.g. evapotranspiration and interaction between storage elements, are not described explicitly in our model, but accounted for by the retrievals and by the weights assigned to antecedent precipitation. Moreover, most of the data required in the three implementations can be derived from satellite observations, e.g. precipitation from Tropical Rainfall Measuring Mission (TRMM) (Huffman et al., 2007), the WSS and inundated area from SSM/I (Shang et al., 2015) and in the future even stream flow by the Surface Water and Ocean Topography (SWOT) mission (Bates et al., 2014; Gleason and Smith, 2014; Paiva et al., 2015).

Overall, our objective is to develop the discrete rainfall-runoff model with the help of the retrievals of the WSS and inundated area from 37 GHz microwave observations and evaluate different implementations of it. The discrete rainfall-runoff model is a lumped hydrological model, developed according to the water balance equation and the redistribution of antecedent precipitation in time. The term “discrete” means the contributions of precipitation in a certain period can be assigned to time intervals of several days or longer. The method applied to retrieve the WSS and inundated area from 37GHz PDBT has been described in detail by Shang et al. (2015). This study aims at evaluating whether a shorter duration of antecedent precipitation yields satisfactory model performance by using the retrievals of WSS and inundated area. There are five sections in this paper: Introduction, Methods, Data and Study Area, Results, Discussion and Conclusion. In the Method section, the derivation of the discrete rainfall-runoff model, its three implementations, the calibration method, metrics of model performance and validation methods (including cross validation) are explained. We applied our model to the middle and upstream reach of Xiangjiang River basin. A short description of the river basin and of model input data is provided in the section Dataset and Study Area, including the retrieval of the WSS and inundated area. In the Result section, the calibration and validation results are illustrated for each implementation. In the Discussion, we evaluated our assumption about the relationship between the model complexity and the duration of antecedent precipitation by comparing the performance of the three model implementations. The estimated weights of antecedent precipitation in the three implementations were analysed to explain differences in model performance.

2. Method

The WSS and inundated area retrieved with 37 GHz PDBT data describe the surface wetness conditions of a catchment. We develop a lumped, conceptual rainfall-runoff model, i.e. the discrete rainfall-runoff model, to directly use this information, based on the regional water balance model in the Budyko framework (Budyko, 1971; Donohue et al., 2007) and the redistribution of precipitation in time (Sect. 2.1). Our model quantifies the contributions of precipitation to a specific runoff during a certain period by using weights. To estimate the weights, a first implementation is developed by estimating the base flow from observed ground water table depth and assuming that the weights are for a given duration of antecedent precipitation (Sect. 2.2). The second implementation is developed by distinguishing a fast (overland flow) and slow runoff (infiltrated flow) components at top surface with the WSS and inundated area (Sect. 2.3) as in the TOPMODEL (Beven and Kirkby, 1979; Sivapalan et al., 1987) and VIC model (Liang et al., 1994; Wood et al., 1992). The third implementation is developed by estimating the potential subsurface flow from the infiltrated flow in the second implementation (Sect. 2.4). These three implementations have increasing complexity, but can be calibrated with the same linear regression method (Sect. 2.5). The metrics applied to evaluate model performance are explained in Sect. 2.5. The calibration and validation methods, including cross validation, are introduced in Sect. 2.6. The retrievals of the WSS and inundated area from 37GHz PDBT data are described in the section Study area and Dataset.

2.1 Discrete rainfall-runoff model

In the Budyko framework (Budyko, 1971; Donohue et al., 2007), the change in the regional soil water storage is the difference between precipitation and outflows, i.e. stream flow and evapotranspiration, during a certain period. The period needs to be longer than the time scale of fluctuations in soil water storage, thus the model describes the quasi-steady-state conditions as in Donohue et al. (2007); Eagleson (1978). This requirement on the duration of antecedent precipitation implies that only precipitations in a certain period influence stream flow. We assume that this duration is constant for observed stream flows. Taking the redistribution of precipitation in a catchment into account, the water balance equation of each antecedent precipitation can be expressed as:

$$P_i = P_{i,t} = SS_{i,t} + SG_{i,t} + \sum_{j=i}^{j=t} FE_{i,j} + \sum_{j=i}^{j=t} FQ_{i,j} \text{ for integers } t, i \text{ and } j\ , t \geq j \geq i \in [t-m, t] \quad (1)$$

where P_i is antecedent precipitation occurring at the i^{th} time step; t is the observation time step and m is the longest duration of antecedent precipitation; $P_{i,t}$ is the P_i in a catchment at the t^{th} time step; $SS_{i,t}$ and $SG_{i,t}$ are parts of P_i stored in soil and ground water respectively at the t^{th} time step; $FE_{i,j}$ and $FQ_{i,j}$ are parts of P_i that were used by evapotranspiration and water discharge respectively at the j^{th} time step; $\sum_{j=i}^{j=t} FE_{i,j}$ and $\sum_{j=i}^{j=t} FQ_{i,j}$ are the cumulated evapotranspiration and cumulated water discharge to rivers due to P_i during the period [i, t].

The VIC model simulates stream flow as the summation of direct runoff from precipitation and base flow from soil layers (Wood et al., 1992). The former one is the contribution of precipitation occurring at the observation time step and the later one integrates the contribution of precipitation in a certain antecedent period. Thus the stream flow observed at t^{th} time step,

i.e. Q_t, can be calculated as the integration of released water flow at this time step due to precipitations in a given antecedent period, i.e. $FQ_{i,t}$, as follow:

$$Q_t = \sum_{i=t-m}^{i=t} FQ_{i,t} \quad (2)$$

Using Eq. (1), Eq. (2) can be expressed as:

$$Q_t = \sum_{i=t-m}^{i=t}\left[P_i - SS_{i,t} - SG_{i,t} - \sum_{j=i}^{j=t} FE_{i,j} - \sum_{j=i}^{j=t-1} FQ_{i,j}\right], \text{ for integers } t, i \text{ and } j, t \geq j \geq i \in [t-m, t] \quad (3)$$

where $i = t$, $\sum_{j=i}^{j=t-1} FQ_{i,j} = 0$. Since $SS_{i,t}$, $SG_{i,N}$, $\sum_{j=i}^{j=t} FE_{i,j}$, and $\sum_{j=i}^{j=t-1} FQ_{i,j}$ are difficult to estimate, the discrete rainfall-runoff model is developed to implement Eq. (8) with precipitation as the only input:

$$Q_t = \sum_{i=t-m}^{i=t} w_i \times P_i \text{ , for integers } t \text{ and } i \text{ , } t > i \in [t-m, t] \quad (4)$$

where

$$w_i = \left(P_i - SS_{i,t} - SG_{i,t} - \sum_{j=i}^{j=t} FE_{i,j} - \sum_{j=i}^{j=t-1} FQ_{i,j}\right)/P_i \quad (5)$$

and the w_i is the weight accounting for the contributions of the i^{th} precipitation to observed stream flow at the t^{th} time step, taking into account the other terms of the catchment water balance. Eq. (4) means that the stream flow at t^{th} time step is due to the contributions of antecedent precipitations during a certain constant period, i.e. $i \in [t-m, t]$. The evapotranspiration and interactions between storage elements are not represented explicitly by the weights, but contribute to determine the weight value. The weights as Eq. (5) shows can have both positive or negative values, which indicate either water discharge (positive value) or recharge (negative value) to stream flow within the whole catchment. The negative values in Eq. (5) indicate the interaction between stream flow and the water storage in a catchment. Stream flow, which is immediately produced by P_i (e.g. overland flow) and slowly produced by P_i stored in soil and ground water (e.g. subsurface and base flows), may recharge soil layers and ground water in the lower reach of a catchment under consideration (Mertes, 1997; Sophocleous, 2002), or be stored in lakes and reservoirs and released later on (Vörösmarty et al., 1996). For example, in the spring, the water table depth is higher than river water level in the upper catchment, i.e. groundwater is released to river, while in the lower catchment, groundwater table depth is lower than the river water level, i.e. stream flow recharges soil and ground water. Human activities intensify the interaction between surface water and subsurface. Irrigation system allocates surface water from rivers and channels to crop land in the lower catchment, so that water flow released from upper catchment is used for evapotranspiration and recharged subsurface and ground water in the lower catchment. Thus negative weight values are one of the important factors in our model.

2.2 The first implementation of the discrete rainfall-runoff model: model calibration and performance

The weights in Eq. (4) can be estimated by calibrating this conceptual model with observed stream flow and precipitation using the linear recursive regression method (Young, 1984), if we know the influence period of antecedent precipitation, i.e. m. In the studies of water balance in a catchment (see e.g. Donohue et al. (2007); Eagleson (1978)), m was normally set as one year. When m is so large, it might lead to the problem of overfitting in our model. To avoid this problem, we reduced the duration of antecedent precipitation by introducing the base flow released by ground water. It is assumed that

precipitation in a long antecedent period influences stream flow through ground water. Based on that, we develop the first implementation of the discrete rainfall-runoff model from Eq. (4) as:

$Q_t = \sum_{i=t-m}^{i=t} w_i \times P_i + Q_t^b$, for integer $t \in [t_1, t_2]$ (6)

where

$Q_t^b = k \times G_t + B$

Q_t^b is the base flow produced from the ground water and estimated using observed groundwater table depth G_t at t^{th} time step as a linear reservoir with a releasing factor, i.e. *k*, plus a constant flow, i.e. *B*; *m* is a constant value that represents the longest duration of antecedent precipitation; t_1 and t_2 are the start and end times of annual time series;. w_i has the same meaning as in Eq. (5). For each *t*, the antecedent precipitation is in the time interval [*t-m, t*]. Thus *m*, i.e. the duration of antecedent precipitation, is an inherent parameter of the model in Eq. (6) and needs to be set before running the model. The weights set, i.e. $[w_{t-m}, w_{t-m+1}, \cdots, w_t]$, is constant for all $t \in [t_1, t_2]$, once the duration of antecedent precipitation, i.e. *m*, is defined, so that Eq.(6) can be calibrated with an annual time series.

As Eq. (6) shows, the ground water reservoir is described by using observed ground water table depth and is only due to precipitations older than the *(t-m)*th time step. In the case that our assumption in the first implementation is not satisfied, the releasing factor and constant flow, i.e. *k* and *B*, in Eq. (6) need to be calibrated to balance the fraction of base flow related to the precipitation events in the time interval [*t-m, t*] with that related to older precipitation events. This indicates that this model describes the fluctuations of the regional ground water table depth, rather than its spatial pattern. . The ground water table depth used by Eq. (6) may not be an accurate the spatial average over the whole catchment, since a limited number of field measurements of ground water table is used to estimate *k* and *B* in this study.

2.3 The second implementation of the discrete rainfall-runoff model

The first implementation was developed by taking the component flow with the slowest response to precipitation, i.e. base flow, into account. The WSS and inundated area describes the water saturation condition at the surface, which determines the partition of precipitation into overland and infiltrated flow (Beven and Kirkby, 1979; Liang et al., 1994; Moore, 1985; Sivapalan et al., 1987; Todini, 1996). The overland and the infiltrated flows are drained by rivers and channels with a different time lag, because the water flow velocity at the surface is faster than that in the soil (Sophocleous, 2002). The overland flow provides a fast way for precipitation to reach river, while the infiltrated flow provides a slow way. The first implementation may be improved, when we specify these component flows, instead of precipitation in Eq. (6). Thus, in the second implementation, we replaced precipitation in Eq. (6) with the two component flows using the fraction of WSS and inundated area as:

$Q_t = \sum_{i=t-m}^{i=t} \beta_i^{21} \times Q_i^O + \sum_{i=t-m}^{i=t} \beta_i^{22} \times Q_i^I + Q_t^b$, for integer $t \in [t_1, t_2]$ (7)

where

$Q_i^O = WS_i \times P_i$

$Q_i^I = (1 - WS_i) \times P_i$

Q_i^O and Q_i^I are the parts of precipitation (i.e. P_i), determined by the fraction of the WSS and inundated area (i.e. WS_i); β_i^{21} and β_i^{22} are the weights of overland (i.e. Q_i^O) and infiltrated flow (i.e. Q_i^I)) at the i^{th} time step, respectively. Both fast and slow subsurface flow is produced by Q_i^I. We did not take interception by the vegetation canopy into account in Eq. (7). Q_i^O and Q_i^I are also redistributed in time by a catchment after they are produced. Thus similar with the redistribution of precipitation in Eq. (1), we can express the redistribution of overland flow, i.e. $Q_{i,t}^O$, over the whole catchment after a certain period of time as:

$Q_i^O = Q_{i,t}^O = OW_{i,t} + OS_{i,t} + OG_{i,t} + \sum_{j=i}^{j=t} OE_{i,j} + \sum_{j=i}^{j=t} OQ_{i,j}$, for integers *t*, *i* and *j* , $t \geq j \geq i \in [t-m, t]$ (8)

where $OW_{i,t}$, $OS_{i,t}$, and $OG_{i,t}$ are parts of Q_i^O stored at the surface (e.g. lake and reservoir), soil layers and ground water respectively at the t^{th} time step; $\sum_{j=i}^{j=t} OE_{i,j}$ and $\sum_{j=i}^{j=t} OQ_{i,j}$ are the cumulated evapotranspiration and cumulated stream flow from Q_i^O during the period [*i*, *t*]. The redistribution of infiltrated flow, i.e.$Q_{i,t}^I$, over the whole catchment after a certain period of time can be expressed as:

$Q_i^I = Q_{i,t}^I = IW_{i,t} + IS_{i,t} + IG_{i,t} + \sum_{j=i}^{j=t} IE_{i,j} + \sum_{j=i}^{j=t} IQ_{i,j}$, for integers *t*, *i* and *j* , $t \geq j \geq i \in [t-m, t]$ (9)

where $IW_{i,t}$, $IS_{i,t}$, and $IG_{i,t}$ are parts of Q_i^I stored at the surface (e.g. lake and reservoir), in soil layers and ground water respectively at the t^{th} time step; $\sum_{j=i}^{j=t} IE_{i,j}$ and $\sum_{j=i}^{j=t} IQ_{i,j}$ are the cumulated evapotranspiration and cumulated stream flow from Q_i^I during the period [*i*, *t*]. According to Eq. (5), the weights of the overland and infiltrated flows can be expressed as:

$\beta_i^{21} = \left(Q_i^O - OW_{i,t} - OS_{i,t} - OG_{i,t} - \sum_{j=i}^{j=t} OE_{i,j} - \sum_{j=i}^{j=t-1} OQ_{i,j}\right)/Q_i^O$ (10)

$\beta_i^{22} = \left(Q_i^I - IW_{i,t} - IS_{i,t} - IG_{i,t} - \sum_{j=i}^{j=t} IE_{i,j} - \sum_{j=i}^{j=t-1} IQ_{i,j}\right)/Q_i^I$ (11)

In Eq. (8) and Eq. (9), evapotranspiration consumes water from both Q_i^O and Q_i^I. Positive weights in Eq. (10) and Eq.(11) mean the component flows contribute to stream flow, while the negative values mean that stream flow recharges water storage.

A very important reason to apply the WSS and inundated area in Eq. (7) is that overland and infiltrated flows, which are produced from the same precipitation event, are collected into stream flow with different time lag, i.e. $\beta_i^{21} \neq \beta_i^{22}$. Accordingly, in the second implementation, the weights of precipitation, i.e. w_i in Eq. (6), can be calculated as:

$w_i = \beta_i^{21} \times WS_i + \beta_i^{22} \times (1 - WS_i)$ (12)

Our second assumption is that it can be better to estimates the w_i with the retrieved WS_i and a relatively shorter duration of antecedent precipitation.

2.4 The third implementation of the discrete rainfall-runoff model

The second implementation partitions precipitation into overland and infiltrated flows. A fraction of the infiltrated flow will result in subsurface flow when it encounters deeper saturated soil layers (Beven and Kirkby, 1979; Beven et al., 1984;

Sivapalan et al., 1987), which we define as potential subsurface flow. The rest of infiltrated flow is stored into soil and ground water and mainly used for evapotranspiration. Model performance might be improved by specifying the potential subsurface flow, instead of the infiltrated flow in the second implementation. We assume that the fraction associated with potential subsurface flow can be scaled linearly with ground water table depth. This assumption implies that the depth of the water saturated soil in deeper layer is linearly related to the ground water table depth, thus the upper and lower boundary wetness conditions of the whole soil layer, i.e. the WSS and inundated area and the ground water table depth, can be used to model the outflow produced from the soil layer (i.e. overland flow and subsurface flow). Based on this assumption, in the third implementation we replace the infiltrated flow in the second implementation (Eq. (7)) with the potential subsurface flow as follows:

$$Q_t = \sum_{i=t-m}^{i=t} \beta_i^{31} \times Q_i^O + \sum_{i=t-m}^{i=t} \beta_i^{32} \times Q_i^S + Q_n^b \qquad (13)$$

where

$$Q_i^S = Q_i^I \times (G_i - G_{min})/(G_{max} - G_{min})$$

i.e. Q_i^S is the potential subsurface flow; β_i^{31} and β_i^{32} are the weights of overland flow and potential subsurface flow (i.e. Q_i^S) at i^{th} time step respectively, which have similar meaning as in Eq. (10) and Eq. (11). Q_i^S is estimated using observations of the ground water table depth (i.e. G_i) scaled by the range between maximum and minimum ground water table depth in each year (i.e. G_{max} and G_{min}).

We will compare β_i^{31} with β_i^{21}, and β_i^{32} with β_i^{22} respectively to evaluate the assumption used in Eq. (13). The precipitation weights can then be calculated from the weights in the third implementation as:

$$w_i = \beta_i^{31} \times WS_i + \beta_i^{32} \times (1 - WS_i) \times (G_i - G_{min})/(G_{max} - G_{min}) \qquad (14)$$

In Eq. (14), the surface wetness conditions (i.e. WS_i) and the ground water table depth (i.e. G_i) are the boundary conditions of water flow in the soil. In the third implementation the description of complicated flow processes such as water flow in the vadose zone and evapotranspiration, is not required to simulate stream flow.

2.5 Model calibration and metrics to evaluate performance

Model Calibration

Once the duration of antecedent precipitation is estimated by setting the parameter *m*, the number of required weights in Eq. (6), (7) and (13) is determined and their values can be estimated by calibration against stream flow. The total number of weights needs to be less than the total number of samples in the annual time series, i.e. *n+1*. The linear least squares method is used to solve such over-determined linear equation, so that the model parameters minimize the difference between observed and modelled stream flows. Taking Eq. (6) as an example, the optimal model parameter values are determined by solving the equation:

$$(\mathbf{X^T X})\beta = \mathbf{X^T Y} \qquad (15)$$

where

$$\mathbf{X} = \begin{bmatrix} P_0 & P_{-1} & \cdots & P_{-m} & G_0 & 1 \\ P_1 & P_0 & \cdots & P_{1-m} & G_1 & 1 \\ \vdots & \vdots & \ddots & \vdots & \vdots & \vdots \\ P_n & P_{n-1} & \cdots & P_{n-m} & G_n & 1 \end{bmatrix}, \beta = \begin{bmatrix} w_t \\ w_{t-1} \\ \vdots \\ w_{t-m} \\ k \\ B \end{bmatrix}, \text{and } \mathbf{Y} = \begin{bmatrix} Q_0 \\ Q_1 \\ \vdots \\ Q_n \end{bmatrix}$$

where matrix **X** includes the observations of precipitation, P_i, ground water table depth, G_i, and a constant water flow valued as 1; the matrix $\boldsymbol{\beta}$ is the weights vector including the weights of precipitation contributions, w_i,, the ground water release parameter, k, and the constant water release parameter, B; the matrix **Y** includes the observations of stream flow, Q_i. In Eq. (15), the precipitation in **X** include the observations in the antecedent year, i.e. [P_{-1}, P_{-2}, …, P_{-m}]. The derivation of Eq. (15) and more detailed information on the linear least squares method can be found in many handbooks, such as Björck (1996); Lawson and Hanson (1974). The same method applies to the second and third implementation forms by replacing the precipitations in the matrix **X** with component flows and extending the matrix $\boldsymbol{\beta}$.

In Eq. (15), the weight vector, $\boldsymbol{\beta}$, are constant for all stream flow observations, but applied to observed precipitations at different times, i.e. the P_i in each row of matrix **X** are different. This means that the volumetric contribution of precipitation to stream flow varies at each time step, although the ratio remains constant. On the other hand, in the matrix **X**, the observation P_i is in the rows from i^{th} to $(i+m)^{th}$ and the column position of the observation P_i changes from 0^{th} to m^{th} according to the row position of the contribution weights of precipitation from w_t to w_{t-m}, i.e. from the 0^{th} to m^{th} row in the matrix $\boldsymbol{\beta}$. This means the precipitation weights in $\boldsymbol{\beta}$ account for the evolution of the contribution of the i^{th} precipitation from time step 0 to $-m$ (negative value means antecedent), with corresponding stream flows at time steps from i to $i+m$. In the Discussion section we interpreted the pattern of weights related to the evolution of contributions of precipitation and component flows to stream flow at different time steps. .

Metrics of model performance

To evaluate the performance of the three implementations in estimating stream flow, we used two metrics:

1. the Nash-Sutcliffe Efficiency (Nash and Sutcliffe, 1970) , i.e. NSE:

$$\text{NSE} = 1 - \sum_{i=0}^{n}(E_i - O_i)^2 / \sum_{i=0}^{n}(O_i - \bar{O})^2 \qquad (16)$$

where E_i and O_i are the model estimated and observed stream flow at i^{th} time step, $\bar{O}$ is the average of measured stream flows, $n+1$ is the total number of observations;

and

2. Relative RMSE (RRMSE):

$$\text{RRMSE} = 100\% \times \sqrt{\sum_{i=0}^{n}(E_i - O_i)^2/(n+1)} \Big/ \bar{O} \qquad (17)$$

NSE indicates how well the model estimates the observed (temporal) signal, while RRMSE is a measure of the bias in the model estimates.

2.6 Model validation

Calibration and Validation

To calibrate and validate the model, the time series of stream flow observations is partitioned into a calibration and validation data set. The model parameters, i.e. the weights in Eq. (15), are estimated first using the calibration data set, then the model is applied to the validation period and is evaluated against the observations in the validation data set. We have calibrated all three implementations for both a dry and wet year to assess the impact of hydrological conditions on model parameters. The model parameters used to predict stream flows are derived from three experiments: 1) a wet year: 2) a dry year; 3) parameters averages over the wet and dry year.

Cross-validation process

The linear regression method as Eq. (15) shows may lead to overfitting the calibration data set, when the number of unknown parameters in the vector $\boldsymbol{\beta}$ is close to the number of total observations in an annual time series, i.e. in the matrix **Y**. To evaluate the overfitting, we used the Leave-One-Out (LOO) method. LOO method removes one sample in stream flow observations, e.g. Q_i in the matrix Y, and its involved precipitation observations, e.g. i^{th} row in the matrix X, from the one-year time series. The model parameters are estimated using the remaining observations and then used to estimate the stream flow observation that has been removed. Thus for an annual time series, ($n+1$) estimates are used for cross-validation. The RRMSE metric was used to evaluate model performance in the cross-validation.

3. Data and Study Area

The study area is the Changsha upstream catchment in the Xiangjiang River basin (blue polygon in Fig. 1), covering 88,125 km^2 and located at 25°12'32.29" N - 28°29'30.11" N and 111°01'10.29" E - 113°52'58.29" E. Mean annual precipitation in this region is around 1700 mm. The rainy season is from April to June. Abundant water resources make the Xiangjiang River basin as one of the best irrigated floodplains in China. Paddy fields consume the largest share of water resources. Many small lakes, wetlands and fish ponds are the natural reservoirs of the river basin. There are also many artificial reservoirs distributed along the tributaries and the main stream of the Xiangjiang River, in order to meet increasing requirements for electrical power from industry and cities.

We used observations of the ground water table depth at 9 wells in Changsha (at the pixel numbered 1 in Fig. 1). Only mean values over 10 days were freely available and were used to calculate the spatially averaged values over this pixel, without knowing the precise location of each observation site, due to the data policy in China. The spatially averaged 10-day mean values in the pixel numbered 1 were used to represent the ground water table depth in the whole study area, since the spatial representation is not so important in our model. The WSS and inundated area, precipitation and stream flow data were also averaged over 10-days. The input data was then 10-day averages of the WSS and inundated area (Fig. 2) over the whole study area, as retrieved with daily 37 GHz PDBT observations according to Shang et al. (2015). In our previous study, the atmosphere influence on PDBT at 37 GHz was removed by a time series analysis method (see Shang et al. (2016)), which

extracts the surface signal from the PDBT time series. The vegetation attenuation of surface emittance was quantified by combining the PDBT observations and Normalized Difference Vegetation Index (NDVI) derived from MODerate-resolution Imaging Spectroradiometer (MODIS). Then, the surface Polarization Difference Effective Emissivity (PDEE) was estimated using a simple radiative transfer model. The fractional WSS and inundated area was derived using a linear model, which uses the PDEE at dry and totally-water-saturated soil to scale the retrieved PDEE. Considering surface roughness in the Xiangjiang River basin, the PDEE of dry and total-water-saturated soil was set as 0.022 and 0.122 respectively. We used the PDBT data at 37 GHz from SSM/I, which is registered in the EASE-Grid with the spatial resolution of 25 km × 25 km (Armstrong et al., 1998). SSM/I is on board the Defense Meteorological Satellite Program (DMSP) satellites, which are sun-synchronous and scan the Earth surface with a constant incident angle of 53 °. Only the early morning overpass data was used to retrieve the fractional area of WSS and inundated area, so that the temperature difference between vegetation canopy and surface could be neglected. Since the discrete rainfall-runoff model is lumped, we calculated the fractional WSS and inundated area over the whole catchment (Fig. 2). The 10-day averages of precipitation data (Fig. 2) were extracted from the ITP-atmosphere forcing data set (Chen et al., 2011; Yang et al., 2010) over the whole study area. This data set is based on the calibration of TRMM precipitation retrievals against rain-gauge data in China. The daily stream flow at the Changsha hydrology station is not affected by water consumed for irrigation and by water storage in the reservoirs. The daily stream flow was also averaged over 10-day (Fig. 2). The 10-day averaged data was used to calibrate and validate the three implementations of the discrete rainfall-runoff model. We have three annual time series of gauged stream flow and ground water table depth, in 2001, 2002 and 2005. 2002 is the wettest year and 2005 the driest year from 2000 to 2006, according the precipitation data. The calibration period was 2002 (wet year) and 2005 (dry year), and the validation period was 2001.

4. Results

4.1 General

The three implementation forms were calibrated with 10-day averaged stream flow at Changsha station in 2002 (wet year) and 2005 (dry year) respectively. The wettest and driest conditions would help us to identify globally optimal parameters. The longest duration of antecedent precipitation was increased step-wise from 1 to 15 time steps, i.e. 10 days to 150 days, in order to evaluate how the model performance would change with the duration of antecedent precipitation. Cross validation was applied to evaluate whether the changes in model performance were due to overfitting. We applied the LOO method to each implementation with various durations of antecedent precipitation for 2002 and 2005 respectively. For annual time series (sampled at 10 days intervals), there were 36 data points useful for cross-validation results for each applied duration.

In addition we evaluated our models with stream flow measurements in 2001 for each implementation. The annual precipitation of 2001 was close to 2002, i.e. a relatively wet year. In the validation process, the model parameters were derived from three experiments: 1) calibration with stream flow in 2002: 2) calibration with stream flow in 2005; 3) parameter averages over 2002 and 2005.

4.2 Simulation with the first implementation of the discrete rainfall-runoff model

4.2.1 Calibration of the first implementation

The first implementation was developed by adding the base flow to the discrete rainfall runoff model and assuming that the weights are constant and only depend on the duration of antecedent precipitation (Eq. 6). The calibration was done against the stream flow in 2002 (wet year) and 2005 (dry year), with the longest duration of antecedent precipitation increasing from 1 to 15 time steps (i.e. from 10 days to 150 days). As the three examples of the simulated stream flows show (Fig. 3), over-estimation occurred after September in 2002 and before September in 2005, and under-estimation occurred in the other months, when the longest duration of antecedent precipitation was 1 time step. In both years a duration of antecedent precipitation between 8 or 15 time steps reduced the bias (Fig. 3).

Model performance was improved in calibration when increasing the longest durations of antecedent precipitation from 1 to 15 time step (Fig. 4 and Fig. 5): the *NSE* of the first implementation increased from 0.78 to 0.91 in 2002 (Fig. 4a) and from 0.82 to 0.94 in 2005 (Fig. 5a), while the RRMSE decreased from 34 % to 22 % in 2002 (Fig. 4b) and from 28 % to 17 % in 2005 (Fig. 5b). The improvement rate, however, was different at various stages: in 2002, the improvement was larger when the duration was increased from 1 to 2 time steps and from 7 to 8 time steps than in the other stages (Fig. 4); in 2005, the largest improvement occurred when the duration was increased from 6 to 7 steps (Fig. 5). The model performance was slightly degraded by increasing the duration from 2 to 7 time steps in 2002 (Fig. 4). These findings suggests that there are some critical key time steps that have a large impact on model performance.

4.2.2 Cross validation of the first implementation

When the duration is increased step-wisely, the number of model parameters also increases. The improvement in model performance may also be related to the overfitting of the linear regression in Eq. (15). To evaluate that, we summarized the RRMSE of all LOO tests for each duration of antecedent precipitation applied in the evaluation of the first implementation (Fig. 6). The RRMSEs clearly varied in a similar range when the duration was increased step-wisely (Fig. 6): the median values in 2002 and 2005 fluctuated between 20 % to 30 % with various durations, i.e. with a different number of weights (model parameters). The mean value slowly increased in 2002, while in 2005 the mean value varied in a similar range as the median values. This means that the overfitting is not the cause of the improvements in model performance of the first implementation.

4.2.3 Validation of the first implementation

The calibrated model parameters were applied in three validation experiments. In these experiments (Fig. 7a), increasing duration of antecedent precipitation did not improve the model performance as significantly as in the calibration experiments. The model performance was improved slightly when the duration was increased from 6 to 9 time steps (Fig. 7a). With the same duration, the experiment 3 (i.e. using parameters averaged over 2002 and 2005) gave the highest NSE ($0.69 \leq NSE \leq 0.82$) and lowest RRMSE ($35.0\ \% \leq RRMSE \leq 58.5\ \%$) than the other two experiments. Both the highest NSE and lowest RRMSE did occur in the experiment 3, but the former with duration = 9 time steps and the latter with duration = 2 time steps

(Table 1). When using the parameters and the durations in Table 1, the stream flow predicted by the first implementation follows the seasonal changes of stream flow very well but overestimates the peaks, especially in the rainy season (Fig. 8a). The predicted stream flow with the duration =2 time steps lagged the peak of the observed stream flow at DOY 121, thus the duration = 9 time steps gives the best performance in the study area with the first implementation. Through the calibration and validation processes, we can conclude that constant weights, i.e. independent of time of year, can be applied when using the base flow to account for older precipitations.

4.3 Simulation with the second implementation of the discrete rainfall-runoff model

4.3.1 Calibration of the second implementation

The second implementation applies two paths for precipitation to reach rivers and channels with the WSS and inundated area (Eq. 7). One is fast overland flow and the other one is slow infiltrated flow. In the calibration of the second implementation, the bias in the stream flow simulated with a duration of 1 time step (Fig. 9) was similar to the bias obtained with the first implementation when using the same duration (Fig. 3). When the duration = 8 time steps, however, the second implementation simulated the stream flow (Fig. 9) as well as the first implementation with the duration = 15 time steps (Fig. 3). This could also be observed from their NSE and RRMSE (Fig. 4 and 5): NSE and RRMSE of the second implementation with the duration = 8 time steps were similar to the first implementation with the duration = 15 time steps. In the calibration experiments, the NSE and RRMSE of the second implementation were better than the first implementation with the same duration (Fig. 4 and Fig. 5). When the duration of antecedent precipitation was increased from 1 to 10 time steps, NSE increased from 0.78 to 0.94 in 2002, from 0. 83 to 0.96 in 2005, and RRMSE decreased from 34 % to 17 % in 2002, from 27 % to 12 % in 2005. The improvement rate was also different in different stages: in 2002, large improvements occurred when the duration was increased from 1 to 3 time steps and from 7 to 9 time steps; in 2005, large improvements occurred when the duration was increased from 2 to 3 time steps and from 6 to 9 time steps. When the duration = 10 time steps, the model performance of the second implementation was better than 90% of current hydrological models in the calibration process, according to the statistical assessment by (Ritter and Muñoz-Carpena, 2013). The performance improvement when the duration > 10 time steps is probably due to the overfitting, as shown next.

4.3.2 Cross validation of the second implementation

The calibration of the second implementation gave very high model performance with duration = 15 time steps. In this case the number of model parameters was close to the total number of stream flow observations. This leads to the problem of overfitting and we evaluated this by applying the LOO method to the second implementation. The box plot of LOO results shows that (Fig. 10): in 2002 with duration ≤10 time steps, both median and mean RRMSE values fluctuated between 20% to 30%; with duration > 10 time steps, median and mean values increased and the 25%-75% variation range was enlarged significantly. In 2005, a similar condition was observed, but the transition duration was longer, i.e. up to time step = 13. This indicates that the overfitting problem occurred when the duration of antecedent precipitation > 10 time steps in the second

implementation. Thus only when the duration ≤ 10, the improved performance is related to the use of the retrieved WSS and inundated area.

4.3.3. Validation of the second model implementation

The validation of the second implementation required more complex experiments. There were three stages in the evolution of NSE with the duration of antecedent precipitation (Fig. 7b): 1) when the duration ≤ 3 time steps, the experiment 1 (i.e. parameters calibrated for 2002) gave the best NSE (0.73 ≤ NSE ≤ 0.84); 2) when 5 < duration ≤ 10 time steps, the experiment 3 (i.e. parameters averaged over 2002 and 2005) had the highest NSE (0.58 ≤ NSE ≤ 0.74); 3) when the duration > 10 time steps, NSE for all experiments was lower than 0.5.

Changes in RRMSE were similar, but with different duration ranges (Fig. 7b): 1) when the duration ≤ 10 time steps, experiment 3 had better RRMSE than the other two, with 32.8% ≤ RRMSE ≤ 66.2%;; 2) when the duration > 10, RRMSE for all experiments was higher than 70 %. Overall, the model performance decreased when the duration increased in the validation experiments. The highest NSE occurred in the experiment 1 with duration = 1 time step, while the lowest RRMSE occurred in the experiment 3 with duration = 1 time steps (Table 1). The stream flows that were predicted by the second implementation using the parameters having the best model performances (Table 1) overestimated the peaks in the rainy season (Fig. 8b), but performed better than the first implementation (Fig. 8a). Thus the second model implementation, the duration = 1 time step gives better results than the first implementation with duration = 9 time steps. This proves that a reasonable model performance can be achieved with a shorter duration of antecedent precipitation when using the retrievals of WSS and inundated area.

4.4 Simulation with the third implementation of the discrete rainfall-runoff model

4.4.1 Calibration of the third implementation

The third implementation estimates the potential subsurface flow from the infiltrated flow derived in the second implementation to specify the path of precipitation through soil layers to rivers and channels. In-situ measurements of the ground water table depth were used to estimate the fraction of infiltrated flow from the potential subsurface flow (Eq. 13). In the calibration experiments, with duration of antecedent precipitation = 1 time step, the error of estimate was (Fig. 11) similar to the other two implementations (Fig. 3 and 9). With duration = 8 and 15 time steps, the accuracy of simulated stream flow in 2002 was better (Fig. 11a) than with the other two implementations (Fig. 3a and Fig. 9a). In 2005, the accuracy of simulated stream flow was comparable with the second implementation. The comparison of NSE and RRMSE (Fig. 4 and Fig. 5) leads to similar conclusions: when the duration was increased from 1 to 10 time steps, the third implementation gave the best performance with NSE increasing from 0.86 to 0.97 in 2002 and from 0. 83 to 0.96 in 2005, while RRMSE decreased from 27 % to 12 % in 2002 and from 27 % to 12 % in 2005. In 2005 the performance of the third and the second implementation was almost the same (Fig. 5).

4.4.2 Cross validation of the third implementation

Likewise the second implementation, the overfitting problem was evaluated for the third implementation. The box plots of LOO results for the third implementation (Fig. 12) show that: in 2002, when the duration ≤10 time steps, both median and mean RRMSE values fluctuated between 20% to 40%, while when the duration > 10 time steps, median and mean values increased with larger quartile ranges; in 2005, a similar condition was observed, but with a longer transition duration at 14 time steps. Overfitting in the third implementation is very similar to the second implementation. Thus only when the duration ≤ 10, performance improvements are related to the application of the potential subsurface flow.

4.4.3. Validation of the third implementation

The validation experiments showed that the model performance was acceptable only when the duration ≤ 10 time steps (Fig. 7c). Experiment 3 had higher NSE ($0.65 \leq NSE \leq 0.82$) and lower RRMSE ($40.1\ \% \leq RRMSE \leq 50.4\ \%$). Overall the influence of the duration of antecedent precipitation in the third implementation was similar to the second implementation, i.e. leading to decreasing model performance with increasing the duration. The highest NSE and lowest RRMSE occurred in the experiment 3 (parameters averaged over 2002 and 2005) with the duration = 1 time step (Table 1). In this experiment the third implementation captured the time of major streamflow peaks correctly, but with larger errors than the second implementation (Fig. 8b and Fig. 8c). Overall, our results show that the potential subsurface flow can be estimated with the retrieved WSS and inundated area and in-situ observations of ground water table depth.

5. Discussion

5.1 Calibration and validation results

The results presented in Sect.4 document the feasibility of calibrating the three model implementations and to achieve a satisfactory performance by using the mean values of parameters calibrated for a wet and a dry year. The three implementations were designed with increasing complexity by specifying the slow and fast component flows produced from precipitation. Our aim was to evaluate whether the increasing complexity could reduce the duration of antecedent precipitation required to achieve a reasonable accuracy. The calibration experiments showed that a short duration of antecedent precipitation gave a model performance with the second and third implementation similar to the first one with a long duration (Fig. 4 and Fig. 5). For example, when the duration of antecedent precipitation = 8 time steps, the simulated stream flow using the second (Fig. 9) and third implementation (Fig. 11) was close to or better than those using the first one with the duration = 15 time steps (Fig. 3). In the calibration experiments the third implementation gave a slightly better model performance than the second one, but the difference was small (Fig. 4 and Fig. 5). The results of cross validation for the three implementations showed when the duration ≤ 100 days, overfitting did not occur in the all three implementation. Thus within this duration range, the model improvement from the first to the second and third implementations was due to the application of the WSS and inundated area. In the validation experiments (Table 1), the first implementation required the duration of 9 time steps to achieve a similar performance as the second and third implementations, which only used the duration of 1 time step. This analysis supports that increasing complexity and applying the retrievals of WSS and inundated

area in the discrete rainfall runoff model reduces the required duration of antecedent precipitation, without degradation of model performance. The second implementation achieved better performance than the other two implementations (Table 1): this indicates that the complexity of the second implementation is enough to simulate and predict stream flow.

The longest duration of antecedent precipitation determines the number of unknown parameters in the matrix $\boldsymbol{\beta}$ in Eq. (15). For a given duration, the second and third implementations require the same number of unknown parameters, while the first implementation requires fewer parameters. Besides the duration of antecedent precipitation, the influence of the number of unknown parameters on the model performance needs to be evaluated. We compared the model performances of the three implementations with the same number of unknown parameters. In the calibration experiments for 2002 (Fig. 13a), the second and third implementations gave better NSE than the first one, except when the number of unknown parameter = 4. In 2005 (Fig. 13b), the situation is opposite: the first implementation gave better NSE than the other two, except when the number of unknown parameter = 8. This large difference between 2002 and 2005 indicates that the WSS and inundated area will be more important in the wet year than in the dry year. The mean parameter values were used to analyse the influence of the number of model parameters in the 2001 validation experiments (Fig. 14), since this set of model parameters gave the best accuracy for all three implementations, compared with the other two experiment sets (Fig. 7). The second implementation had better NSE than the other two when the number of unknown parameters = 4 and the third one had better NSE than the other two when the number of unknown parameters = 6. When the parameter number $\geq$ 8, the first implementation had the best NSE. With parameter number $\leq$ 6, the NSEs of the second and third implementations were similar to the NSE of the first implementation with parameter number $\geq$ 8 (Fig. 14). In other words, comparable accuracy was achieved when using the retrievals of WSS and inundated area and fewer model parameters.

5.2 The performance of the three implementations with the mean model parameters

In the validation experiments, the best performance for all three implementations was obtained when using the parameter values averaged over the wet (2002) and dry (2005) (Fig. 7 and Table 1). In Table 1, we also listed the longest durations of antecedent precipitation applied to achieve the best performance with each implementation. The averaged parameters and the corresponding durations in Table 1 can also be used to predict the stream flow in 2002 and 2005 to evaluate the performance of the three implementations, since they are different from the ones obtained by calibration for each year. For the first implementation, we applied the averaged parameters and the duration of 9 time steps, while for the second and third implementation we applied the averaged parameters and a duration of 1 time step. The first and second implementations gave similar estimates of stream flow (Fig. 15). Streamflow was underestimated between DOY 100 and 240 in 2002, and between DOY 200 and 260 days in 2005, while it was overestimated between DOY 240 and 365 in 2002, and between DOY 160 and 180 in 2005. The performance metrics for the first and second implementations using averaged parameters and the chosen durations were also similar, with $0.77 \leq NSE \leq 0.80$ and $34\% \leq RRMSE \leq 36\%$ in 2002 and $0.78 \leq NSE \leq 0.79$ and RRMSE=33% in 2005 (Table 2). The third implementation had the best performance in 2002 (with NSE = 0.83 and RRMSE = 31 %) but worst in 2005 (with NSE = 0.67 and RRMSE = 43%). These results suggest that the first and second

implementations have a relative stable performance with the averaged parameters and the chosen durations, while the performance of the third implementation was very different in the dry and wet year.

5.3 Interpretation of the weight set

In calibration experiments, model performances of three implementations were improved by increasing the duration of antecedent precipitation, especially for the second and third implementations. Cross validation results proved that when the duration ≤ 100 days, these performance improvements were due to antecedent precipitations contributing to stream flow production, not due to the increment of model parameters. In the validation experiments, the model performance of the first implementation was slightly improved by increasing the duration, while the performances of the second and third implementations were overall degraded. This difference in the responses of model performance to the durations between the first and the other two implementations is probably due to that the weight range of antecedent precipitations.

The weight set indicates the evolution of the contributions of precipitation or the component flow to stream flows at various time steps during a certain period. The variability in the model performance of three implementations can be explained by analysing the estimated weights. We found that when the duration of antecedent precipitation was increased, the weights in the first implementation (Fig. 16) varied in a smaller range than the weights in the second and third implementations (Fig. 17 and Fig. 18). In the first implementation, the 25%-75% range of precipitation weights varies between 0.01 to 0.1 in 2002 and 0.005 to 0.05 in 2005 (Fig. 16). Due to that the overfitting problems occurred in the second and third implementations when the duration > 10 time steps, we only analysed the weight applying to duration ≤ 10 time steps. In the second implementation, the 25% - 75 % range of weights in overland flow was 0. 1 to 0.4 in 2002 and 0.05 to 0.35 in 2005, while the 25%-75% range of weights in infiltrated flow was 0.05 to 0.3 in 2002 and 0.02 to 0.18 in 2005. In the third implementation form, the range of weights in component flows was similar to that in the second implementation. The small range in the first implementation means that the weights are not so sensitive to the duration of antecedent precipitation as in the second and third implementations. This may explain why in the calibration and validation experiments the performance of the first implementation fluctuated in a small range. The large weight ranges in the second and third implementations yielded faster model improvement than in the first implementation in the calibration experiments (Fig. 4 and Fig 5). But the high sensitivity of the weights to the duration of precipitation and the significant inter-annual variability in the weights (see the analysis below) resulted in the degraded performance of the second and third implementations in the validation experiments.

The weights in the first implementation explain how the catchment responds to rainfalls: positive weights account for water discharge to rivers and channels, while negative weights account for water recharge by stream flow. We found a clear difference in the weights of precipitation (first implementation) between 2002 and 2005 (Fig. 16): in 2002 (wet year, Fig. 16a), a large fraction of precipitation contributed to stream flows after 10, 20, 40 and 70 days, since higher positive weights occur at antecedent time steps of 1, 2, 4, and 7; while in 2005(dry year, Fig. 16b), a large fraction of precipitation contributed to stream flow after 70 days, since high positive weights occur at the antecedent time steps of 0 and 7. The second and third implementations estimate component flows from precipitation, i.e. specify the paths of precipitation into

rivers and channels. Thus the weights spaces of component flows in the second and third implementations help to interpret how the precipitation contributes to stream flow. For example, after 10 days in 2002, precipitation contributed to stream flow mainly through fast subsurface flow, since the infiltrated and potential subsurface flows both had large positive weights at the time step of 1 and the mean and median weights of the overland flow were close to 0 (Fig. 17 a, b and Fig. 18 a, b). After 70 days in both 2002 and 2005, we found that precipitation contributed to stream flow through both overland and slow subsurface flows, since the median and mean weights of both overland and potential subsurface flow (infiltrated flow) were positive at the time step of 7 (Fig. 17 and Fig. 18). After 70 days, slow subsurface flow is associated with the release of soil water and overland flow may be associated with the release of water in lakes and reservoirs, e.g. the stream flow mechanism in South America (Vörösmarty et al., 1989; Vörösmarty et al., 1996), where the large inundated forest area releases surface runoff gradually. Thus the precipitation weight is a combination of the weights of the component flows as Eq. (12) and Eq. (14) show. Even without taking the storage of surface water into account, overland flow does not immediately reach river and channels, due to the various routes of surface runoff, which best described by distributed hydrological models, e.g. TOPMODEL (Beven et al., 1984). In a wet year (Fig. 17a), overland flow is gradually released for 50 days after rainfall, which is close to 1.5 month time lag between precipitation and stream flow in a large catchment as observed by (Gleick, 1987).

Another interesting difference between 2002 and 2005 is the precipitation contribution at 0 time step, i.e. when it falls on the catchment. When rain falls in 2002, precipitation contributed to stream flow mainly through overland flow, since the overland flow at 0 time step had large positive weights in the second (Fig. 17a) and third (Fig. 18a) implementations, while the produced infiltrated flow, had been used to recharge soil layers, since the infiltrated and potential subsurface flow both had negative weights (Fig. 17b and Fig. 18b). In 2005, an opposite situation occurs: the overland flow was used to recharge soil layers, i.e. negative mean and median weights in overland flow at 0 time step (Fig. 17c and Fig. 18c), while fast subsurface flow reached rivers, i.e. positive mean and median weights in infiltrated ((Fig. 17d)) and potential subsurface flow (Fig. 18d). This difference is mainly related to the different soil wetness condition in wet and dry years. In 2002, water saturation condition in the top soil layer was high, thus a large fraction of precipitation was used to produce overland flow. I In 2005, top soil layer was dry, thus a large fraction of precipitation percolated into deep soil and produced fast subsurface flow.

In 2005, the weights of overland flow in the third implementation form (Fig. 18c) were almost the same as in the second implementation form (Fig. 17c), and the weights of potential subsurface flow in the third implementation (Fig. 18d) were very similar to the ones of infiltrated flow in the second implementation (Fig. 17d). This means that the potential subsurface flow in combination with observed groundwater table is an effective schematization of hydrological processes in the study area.

5.4 The recharge period of ground water

In the calibration period, there were some stages when the model performance was improved much more than in other cases (Fig. 4 and Fig. 5). This indicates that specific time steps have larger impacts on the model performance than others. In the validation experiments, we found that when the time step was increased from 6 to 9, the model performance was improved in all three implementations using the parameters in the three experiments. Thus we calculated the RRMSE in each season of both 2002 and 2005 for the three implementations with various durations (Fig. 19). When the duration was increased from 1 to 15 time steps, the reduction in RRMSE was significant in the autumn and winter for the first implementation (Fig. 19a). This indicates that the stream flow after June is influenced by longer antecedent precipitations, for example those in the spring. This is consistent with other studies on the floods in this river basin (Lin and Lu, 1991; Zhou, 1991; Zong and Chen, 2000), where the magnitude of floods after June was related to the rain in the spring. In the autumn and winter for the first implementation (Fig. 19a) and in all four seasons for the second and third implementations (Fig. 19b and 19c), when the longest duration < 8 or 9 time steps, RRMSEs were much higher than those with the longest durations ≥ 8 or 9 time steps. When increasing the longest duration range from 8 or 9 time steps to 15 time steps, the RRMSE in each season improved slightly for all three implementations. This gives an estimate of time needed for precipitation to recharge ground water in our study area, i.e. 80 or 90 days, since all three implementation forms are based on the assumption that base flow is only from precipitations older than a certain time.

Conclusions

The retrievals of the Water Saturated Soil (WSS) and inundated area from 37GHz microwave observation (Shang et al., 2015) supplies a straightforward and lagged relationship between precipitation and stream flow. To fully and effectively use this data, we developed a discrete rainfall-runoff model based on the water balance at the whole catchment and the redistribution of precipitation in time. This model simulates the stream flow as the weighted sum of precipitations during a certain constant antecedent period. The three implementations have increasing complexities. The first implementation was developed using base flow to replace older precipitation. The second implementation was developed by estimating the overland (fast) and infiltrated (slow) flow from precipitation using the retrievals of the WSS and inundated area with PDBT at 37 GHz. The third implementation form was developed by estimating the potential subsurface flow from the infiltrated flow.

Through calibration and validation, the three implementations were proved to be able to estimate stream flows in the Xiangjiang river basin, China. The longest duration of precipitation is an important factor to determine model performance. In the calibration experiments, 10-day mean stream flows at Changsha station in 2002 (wet) and 2005 (dry) are used to estimate the weights with various durations. Increasing the longest duration from 1 to 10 time steps, the NSE of the first implementation increased from 0.78 to 0.86 in 2002, from 0. 82 to 0.92 in 2005, and RRMSE decreased from 34 % to 27 % in 2002, from 28 % to 19 % in 2005. NSE for the second implementation increased from 0.78 to 0.94 in 2002, from 0. 83 to

0.96 in 2005, and RRMSE decreased from 34 % to 17 % in 2002, from 27 % to 12 % in 2005. NSE for the third implementation form increased from 0.86 to 0.97 in 2002, from 0. 83 to 0.96 in 2005, and RRMSE decreased from 27 % to 12 % in 2002, from 27 % to 12 % in 2005. Through cross-validation, it was proved that the increment in model performance is mainly due to the model structure, especially taking the WSS and inundated area and the ground water table depth into account, with the duration ≤ 10 time steps. In the validation experiments, the longest duration used in the second and third implementation should be less than 20 days, much less than for the first implementation, which used 90 days. The mean parameters over 2002 and 2005 gave a stable model performance with the first and second implementations. The complexity level of the second implementation was sufficient to simulate and predict stream flows in the study area.

The pattern of precipitation weights in the first implementation explains the interactions between catchment and stream flow. Clear differences in the catchment response were observed between the dry and wet years. The weights spaces of component flows in the second and third implementation specify the path of precipitation towards stream flow. The range of weights in the first implementations was smaller than in the other two implementations, which probably explained why the first implementation was not so sensitive to the increasing duration of precipitation as the second and third implementations. The weights of overland and potential subsurface flows in the third implementation had a very similar pattern with those of overland and infiltrated flows in the second one, when the depth of water saturated soil was deeper and close to the depth of the groundwater table, e.g. in dry years.

The changes in the RRMSE in autumn for the first implementation indicate the influence of rain in the spring on stream flow in autumn (Lin and Lu, 1991; Zhou, 1991; Zong and Chen, 2000). The changes in RRMSE in each season for the three implementations lead to estimate the duration of ground-water recharge by precipitation at around 90 days. Overall, with the WSS and inundated area as an essential parameter, the three implementations of the discrete rainfall-runoff model not only simulated and predicted stream flow, but also characterized the catchment response to precipitation and the mechanisms determining stream flow. The application of the WSS and inundated area can make the discrete rainfall-runoff model to use fewer parameters.

Acknowledgements:

This paper is supported by the Ministry of Science and Technology of the People's Republic of China (Grant no. 2015CB953702), the SAFEA Recruitment Program of Foreign Experts (also called 1000 Talents Plan, Grant no. WQ20141100224), and the EU-FP7 CEOP-AEGIS project (Grant no. 212921). This investigation is a cooperative effort of the Delft University of Technology, Delft, The Netherlands and the State Key laboratory of Remote Sensing Science, Institute of Remote Sensing and Digital Earth, Chinese Academy of Sciences, Beijing, China. We would like to thank our data providers: Dr. Weiguo Jiang and Dr. Zhigang Liu of Beijing Normal University, Pro. Zhenghui Xie from the Institute of Atmospheric Physics, Chinese Academy of Sciences, and M.Sc. Ming Yin from the Institute of Geo-Environmental Monitoring, China. Without their support, we could not have carried out this study.

References

Armstrong, R., Knowles, K., Brodzik, M., and Hardman, M. A.: DMSP SSM/I-SSMIS Pathfinder Daily EASE-Grid Brightness Temperatures. Version 2. Boulder, Colorado USA: NASA DAAC at the National Snow and Ice Data Center, 1998.

Babyak, M. A.: What you see may not be what you get: a brief, nontechnical introduction to overfitting in regression-type models, Psychosomatic medicine, 66, 411-421, 2004.

Bates, P. D., Neal, J. C., Alsdorf, D., and Schumann, G. J.-P.: Observing global surface water flood dynamics, Surveys in Geophysics, 35, 839-852, 2014.

Beven, K. and Kirkby, M.: A physically based, variable contributing area model of basin hydrology/Un modèle à base physique de zone d'appel variable de l'hydrologie du bassin versant, Hydrological Sciences Journal, 24, 43-69, 1979.

Beven, K., Kirkby, M., Schofield, N., and Tagg, A.: Testing a physically-based flood forecasting model (TOPMODEL) for three UK catchments, Journal of Hydrology, 69, 119-143, 1984.

Björck, A.: Numerical methods for least squares problems, Siam, 1996.

Budyko, M. I.: Climate and life, 1971. 1971.

Chen, Y., Yang, K., He, J., Qin, J., Shi, J., Du, J., and He, Q.: Improving land surface temperature modeling for dry land of China, Journal of Geophysical Research: Atmospheres (1984–2012), 116, 2011.

Donohue, R., Roderick, M., and McVicar, T.: On the importance of including vegetation dynamics in Budyko's hydrological model, Hydrology and Earth System Sciences Discussions, 11, 983-995, 2007.

Eagleson, P. S.: Climate, soil, and vegetation: 1. Introduction to water balance dynamics, Water Resources Research, 14, 705-712, 1978.

Gleason, C. J. and Smith, L. C.: Toward global mapping of river discharge using satellite images and at-many-stations hydraulic geometry, Proceedings of the National Academy of Sciences, 111, 4788-4791, 2014.

Gleick, P. H.: The development and testing of a water balance model for climate impact assessment: modeling the Sacramento basin, Water Resources Research, 23, 1049-1061, 1987.

Gupta, H. V., Sorooshian, S., and Yapo, P. O.: Status of automatic calibration for hydrologic models: Comparison with multilevel expert calibration, Journal of Hydrologic Engineering, 4, 135-143, 1999.

Hawkins, D. M.: The problem of overfitting, Journal of chemical information and computer sciences, 44, 1-12, 2004.

Hayashi, M., van der Kamp, G., and Rudolph, D. L.: Water and solute transfer between a prairie wetland and adjacent uplands, 1. Water balance, Journal of Hydrology, 207, 42-55, 1998.

Huffman, G. J., Bolvin, D. T., Nelkin, E. J., Wolff, D. B., Adler, R. F., Gu, G., Hong, Y., Bowman, K. P., and Stocker, E. F.: The TRMM multisatellite precipitation analysis (TMPA): Quasi-global, multiyear, combined-sensor precipitation estimates at fine scales, Journal of Hydrometeorology, 8, 38-55, 2007.

Jakeman, A. and Hornberger, G.: How much complexity is warranted in a rainfall-runoff model?, Water resources research, 29, 2637-2649, 1993.

Jakeman, A., Littlewood, I., and Whitehead, P.: Computation of the instantaneous unit hydrograph and identifiable component flows with application to two small upland catchments, Journal of hydrology, 117, 275-300, 1990.

Kazezyılmaz-Alhan, C. M., Medina, M. A., and Richardson, C. J.: A wetland hydrology and water quality model incorporating surface water/groundwater interactions, Water Resources Research, 43, 2007.

Lakshmi, V., Wood, E. F., and Choudhury, B. J.: Evaluation of Special Sensor Microwave/Imager satellite data for regional soil moisture estimation over the Red River basin, Journal of Applied Meteorology, 36, 1309-1328, 1997a.

Lakshmi, V., Wood, E. F., and Choudhury, B. J.: A soil-canopy-atmosphere model for use in satellite microwave remote sensing, Journal of Geophysical Research D: Atmospheres, 102, 6911-6927, 1997b.

Lawson, C. L. and Hanson, R. J.: Solving least squares problems, SIAM, 1974.

Liang, X., Lettenmaier, D. P., Wood, E. F., and Burges, S. J.: A simple hydrologically based model of land surface water and energy fluxes for general circulation models, JOURNAL OF GEOPHYSICAL RESEARCH-ALL SERIES-, 99, 14,415-414,415, 1994.

Lin, C. and Lu, J.: Studies on the anomaly of Plum Rain and flood disaster in the Yangtze River valley, J. Najing University, 1991. 76-83, 1991.

Madsen, H.: Automatic calibration of a conceptual rainfall–runoff model using multiple objectives, Journal of hydrology, 235, 276-288, 2000.

Mertes, L. A.: Documentation and significance of the perirheic zone on inundated floodplains, Water Resources Research, 33, 1749-1762, 1997.

Moore, R.: The PDM rainfall-runoff model, Hydrology and Earth System Sciences Discussions, 11, 483-499, 2007.

Moore, R.: The probability-distributed principle and runoff production at point and basin scales, Hydrological Sciences Journal, 30, 273-297, 1985.

Nash, J. E. and Sutcliffe, J. V.: River flow forecasting through conceptual models part I — A discussion of principles, Journal of Hydrology, 10, 282-290, 1970.

Paiva, R. C., Durand, M. T., and Hossain, F.: Spatiotemporal interpolation of discharge across a river network by using synthetic SWOT satellite data, Water Resources Research, 51, 430-449, 2015.
Ritter, A. and Muñoz-Carpena, R.: Performance evaluation of hydrological models: Statistical significance for reducing subjectivity in goodness-of-fit assessments, Journal of Hydrology, 480, 33-45, 2013.
Shang, H., Jia, J., and Menenti, M.: Analyzing the Inundation Pattern of the Poyang Lake floodplain by Passive Microwave Data, Journal of Hydrometeorology, 16, 652-667, 2015.
Shang, H., Jia, J., and Menenti, M.: Modeling and Reconstruction of Time Series of Passive Microwave Data by Discrete Fourier Transform Guided Filtering and Harmonic Analysis, Remote Sensing, 08, 970, 2016.
Shjeflo, J. B.: Evapotranspiration and the water budget of prairie potholes in North Dakota, US Government Printing Office, 1968.
Sippel, S. J., Hamilton, S. K., Melack, J. M., and Novo, E. M. M.: Passive microwave observations of inundation area and the area/stage relation in the Amazon River floodplain, International Journal of Remote Sensing, 19, 3055-3074, 1998.
Sivapalan, M., Beven, K., and Wood, E. F.: On hydrologic similarity: 2. A scaled model of storm runoff production, Water Resources Research, 23, 2266-2278, 1987.
Sophocleous, M.: Interactions between groundwater and surface water: the state of the science, Hydrogeology journal, 10, 52-67, 2002.
Su, M., Stolte, W., and Van der Kamp, G.: Modelling Canadian prairie wetland hydrology using a semi-distributed streamflow model, Hydrological Processes, 14, 2405-2422, 2000.
Temimi, M., Leconte, R., Brissette, F., and Chaouch, N.: Flood and soil wetness monitoring over the Mackenzie River Basin using AMSR-E 37 GHz brightness temperature, 25-29 July 2005 2005, 4 pp.
Todini, E.: The ARNO rainfall—runoff model, Journal of Hydrology, 175, 339-382, 1996.
Vörösmarty, C. J., Moore, B., Grace, A. L., Gildea, M. P., Melillo, J. M., Peterson, B. J., Rastetter, E. B., and Steudler, P. A.: Continental scale models of water balance and fluvial transport: an application to South America, Global biogeochemical cycles, 3, 241-265, 1989.
Vörösmarty, C. J., Willmott, C. J., Choudhury, B. J., Schloss, A. L., Stearns, T. K., Robeson, S. M., and Dorman, T. J.: Analyzing the discharge regime of a large tropical river through remote sensing, ground-based climatic data, and modeling, Water Resources Research, 32, 3137-3150, 1996.
Winter, T. C. and Rosenberry, D. O.: The interaction of ground water with prairie pothole wetlands in the Cottonwood Lake area, east-central North Dakota, 1979–1990, Wetlands, 15, 193-211, 1995.
Winter, T. C. and Valk, A.: Hydrologic studies of wetlands in the northern prairie, Northern prairie wetlands., 1989. 16-54, 1989.
Woo, M.-K. and Rowsell, R. D.: Hydrology of a prairie slough, Journal of Hydrology, 146, 175-207, 1993.
Wood, E. F., Lettenmaier, D. P., and Zartarian, V. G.: A land-surface hydrology parameterization with subgrid variability for general circulation models, Journal of Geophysical Research: Atmospheres (1984–2012), 97, 2717-2728, 1992.
Xu, C.-Y. and Singh, V. P.: Review on regional water resources assessment models under stationary and changing climate, Water Resources Management, 18, 591-612, 2004.
Yang, K., He, J., Tang, W., Qin, J., and Cheng, C. C.: On downward shortwave and longwave radiations over high altitude regions: Observation and modeling in the Tibetan Plateau, Agricultural and Forest Meteorology, 150, 38-46, 2010.
Young, P.: Recursive estimation and time-series analysis: an introduction, 1984. 1984.
Zhao, R.: Flood forecasting method for humid regions of China, East China College of Hydraulic Engineering, Nanjing, 1977. 19-51, 1977.
Zhao, R.: Watershed hydrological modelling, Water Resources and Electric Power Press, Beijing, 1984. 1984.
Zhou, Z.: Synoptic characteristics of atmoshperic cirulation during abnormal Plum Rain period in 1991, J. Nanjing University, 1991. 84-93, 1991.
Zong, Y. and Chen, X.: The 1998 flood on the Yangtze, China, Natural Hazards, 22, 165-184, 2000.

Table 1, The best model performances, their experiment types and the used duration in the 2001 validation for each implementation of the discrete rainfall-runoff model.

		NSE	RRMSE	Used Parameter	Duration
First Implementation	Highest NSE	0.83	35.40%	average	9 time steps
	Lowest RRMSE	0.82	34.10%	average	2 time steps
Second Implementation	Highest NSE	0.84	32.89%	2002	1 time step
	Lowest RRMSE	0.83	32.83%	average	1 time steps
Third Implementation	Highest NSE	0.82	40.05%	average	1 time step
	Lowest RRMSE	0.82	40.05%	average	1 time step

Table 2, Model performance in predicting stream flow in 2002 and 2005 with the three implementations and the mean parameters.

	2002		2005	
	NSE	RRMSE	NSE	RRMSE
1st implementation	0.80	34%	0.78	33%
2nd implementation	0.77	36%	0.79	33%
3rd implementation	0.83	31%	0.67	43%

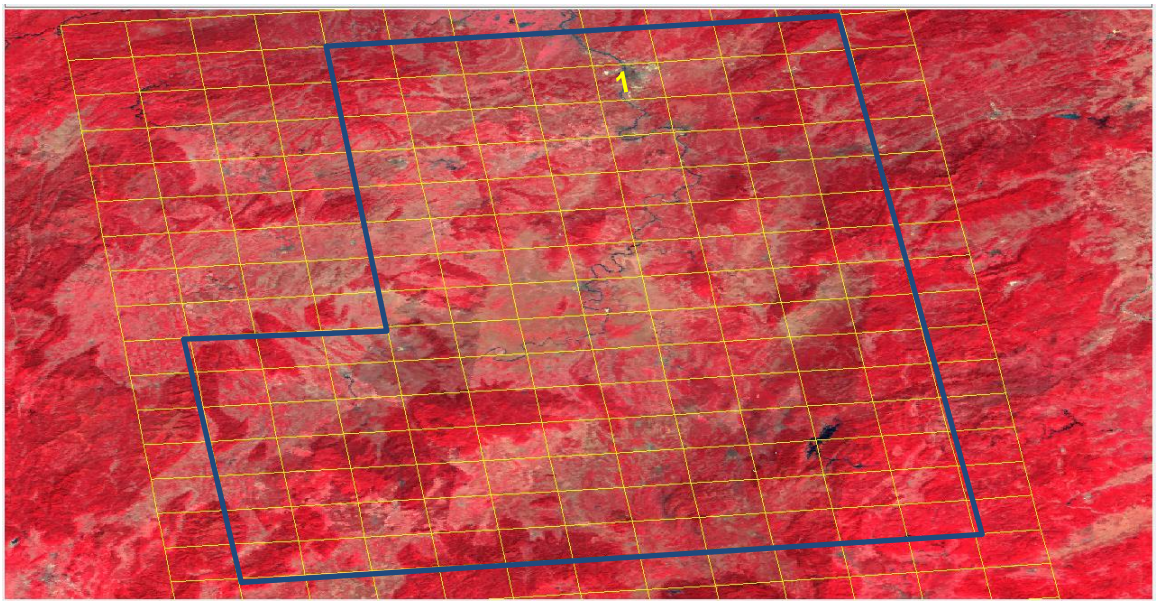

Figure 1: The study area in the middle and upstream of Xiangjiang river basin, China. The blue polygon covers the whole study area. The yellow grid is the 25km×25km EASE-Grid. Background image: RGB composite of MOIDS near-infrared, red and green spectral bands. The wells that measure ground water table depths are located within the yellow pixel numbered with 1.

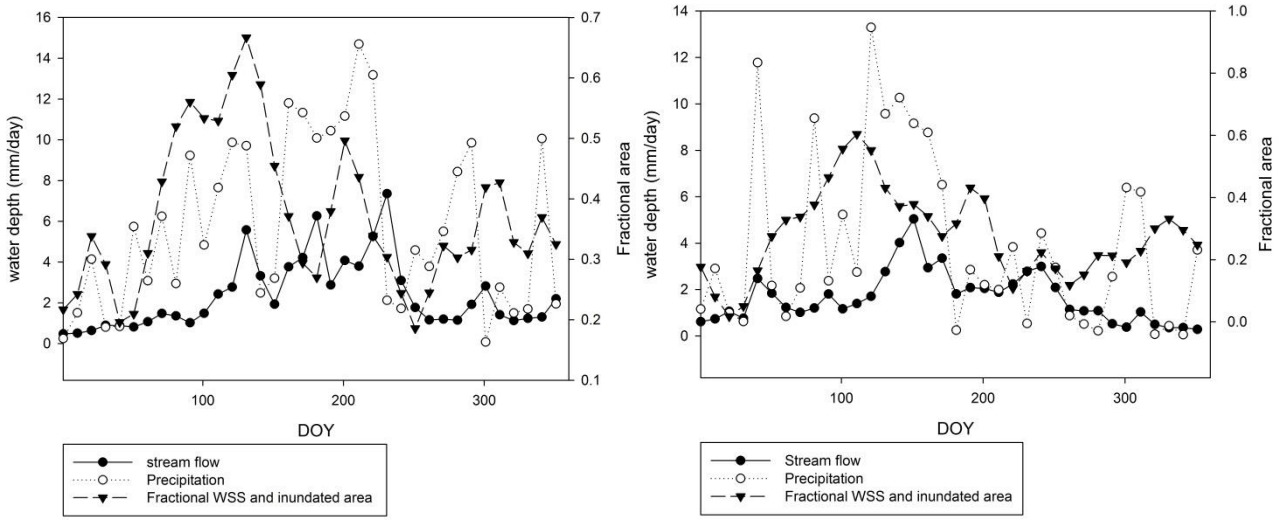

Figure 2: Major input data for the discrete rainfall-runoff model. Precipitation (10-day averages) was extracted from ITP forcing data set (Chen et al., 2011; Yang et al., 2010), fractional WSS and inundated area was retrieved from SSM/I 37GHz PDBT data, and the 10-day averaged stream flow was observed at Changsha station, in 2002 (a) and 2005 (b), respectively.

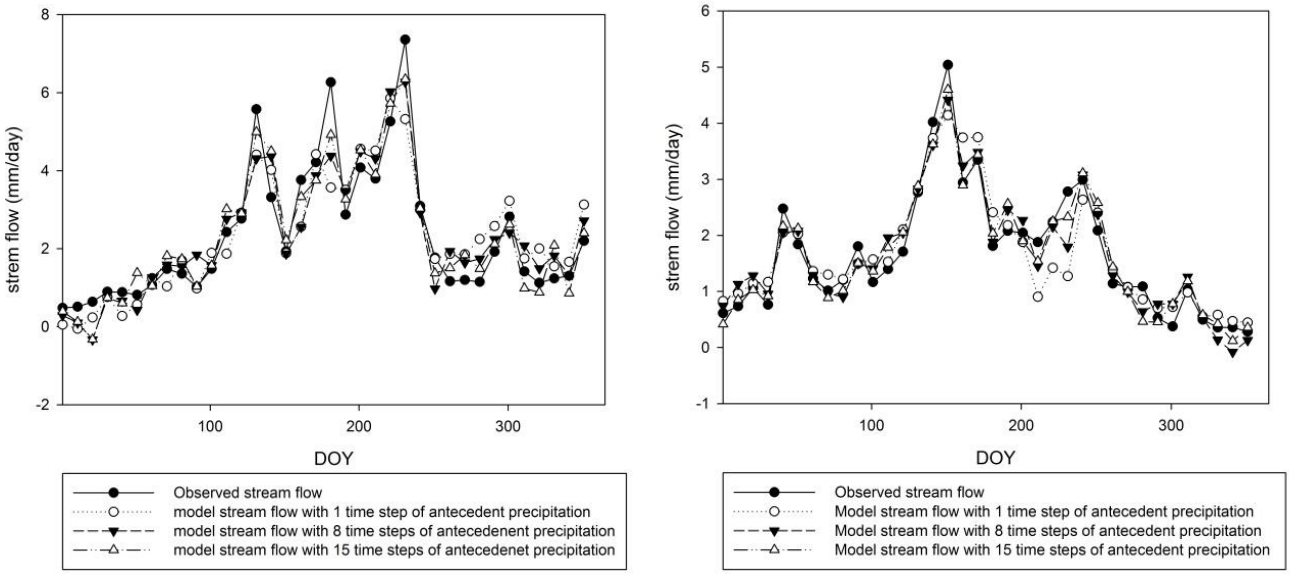

(a) **(b)**

Figure 3: Observed and modelled stream flow using the first implementation of the discrete rainfall-runoff model. The applied durations of antecedent precipitation are 1, 8 and 15 time steps with the time interval of 10 days in 2002 (a) and 2005 (b) respectively.

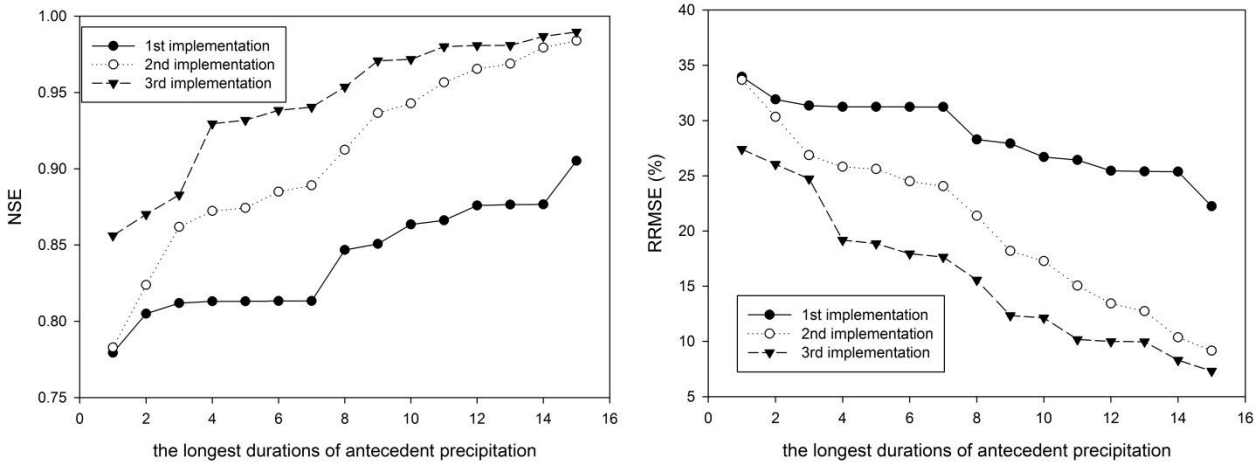

(a) **(b)**

Figure 4: The Nash--Sutcliffe Efficiency (NSE) (a) and Relative Root Mean Square Error (RMSE) (b) of the three implementations of the discrete rainfall-runoff model in the calibration for 2002. The duration of antecedent precipitation were increased from 1 to 15 time steps with time interval of 10 days. The input of the first implementation is precipitation and base flow; the input of the second implementation is overland flow, infiltrated flow and base flow; the input of the third implementation is overland flow, potential subsurface flow and base flow.

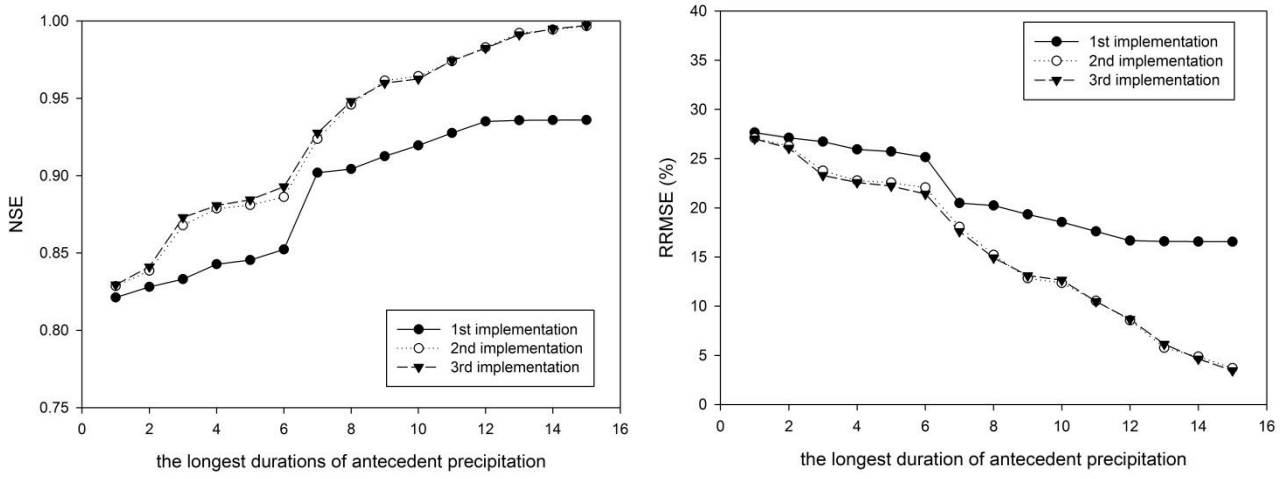

(a) **(b)**

Figure 5: The Nash--Sutcliffe Efficiency (NSE) (a) and Relative Root Mean Square Error (RMSE) (b) of the three implementations of the discrete rainfall-runoff model in the calibration for 2005. The duration of antecedent precipitation were increased from 1 to 15 time steps with time interval of 10 days. the input of the first implementation is precipitation and base flow; the input of the second implementation is overland flow, infiltrated flow and base flow; the input of the third implementation is overland flow, potential subsurface flow and base flow.

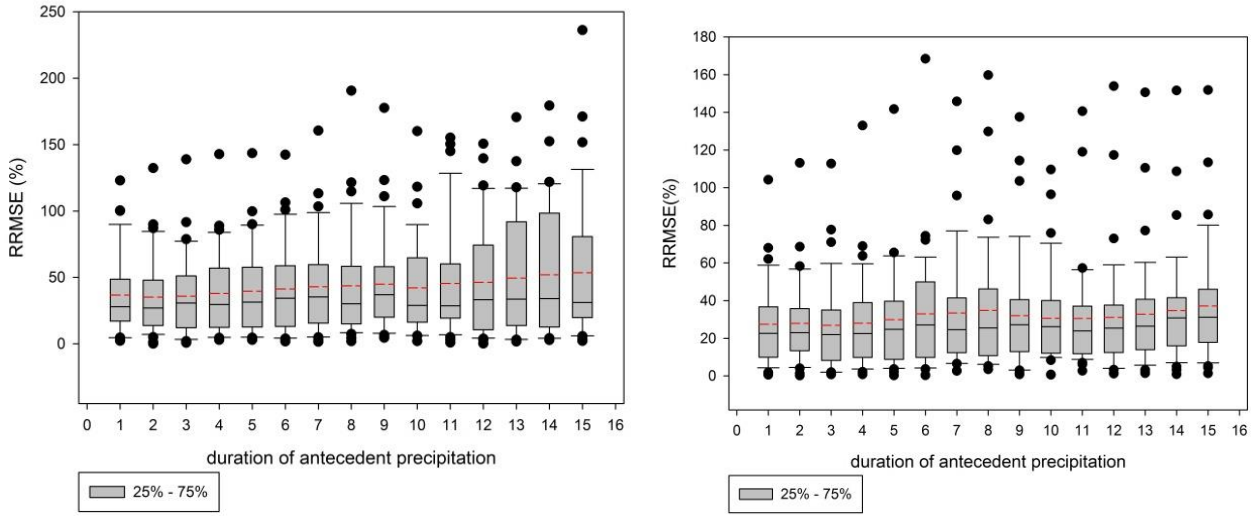

(a) **(b)**

Figure 6: The box plot of the Relative Root Mean Square Error (RRMSE) of the Leave-One-Out cross validation for the first implementation in 2002 (a) and 2005 (b). The duration of antecedent precipitation were increased step-wisely from 1 to 15 time steps with time interval of 10 days. The red dash line in each box is the mean value and the black line is the media value.

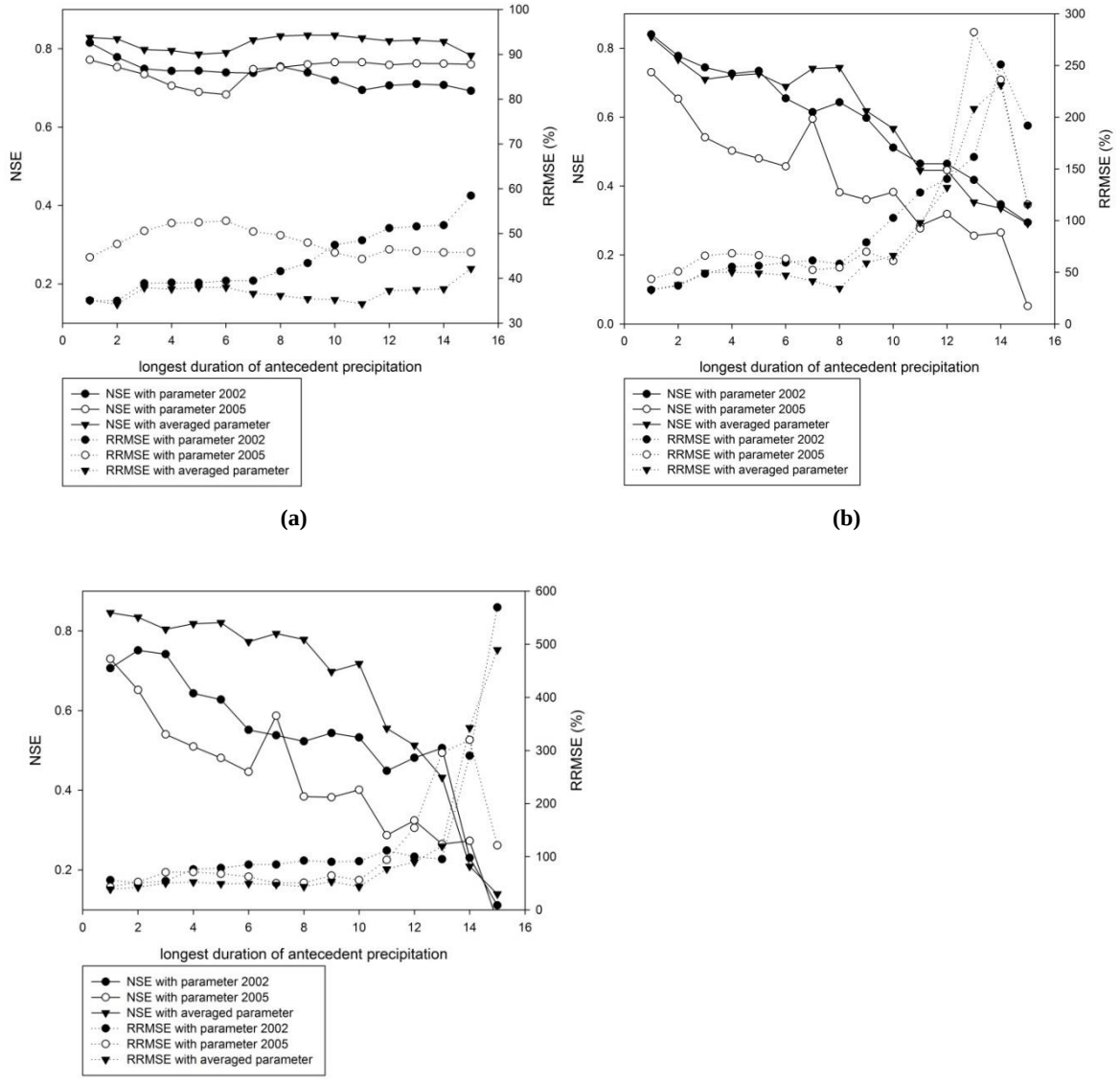

Figure 7: The Nash--Sutcliffe Efficiency (NSE) and Relative Root Mean Square Error (RMSE) of the three implementation in the 2001 validation. a) the first implementation; b) the second implementation; c) the third implementation. Three experiments are designed as: 1) parameters from calibration of 2002; 2) parameters from calibration of 2005; 3) parameters averaged over 2002 and 2005. The duration of antecedent precipitation were increased step-wisely from 1 to 15 time steps with time interval of 10 days. :

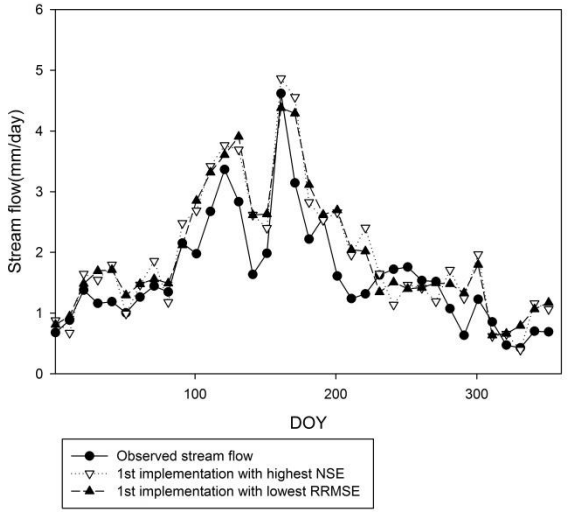

(a)

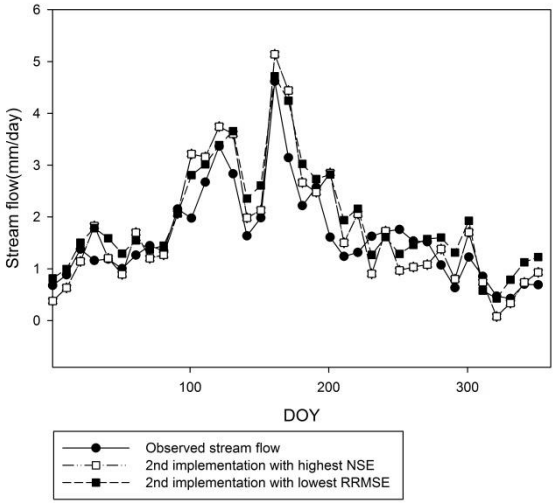

(b)

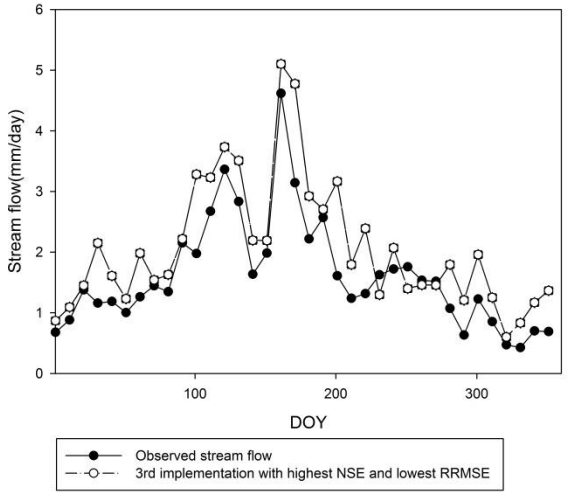

(c)

Figure 8, observed and predicted stream flow in 2001, with the three implementation using the parameters in Table 1: a) the first implementation; b) the second implementation; c) the third implementation.

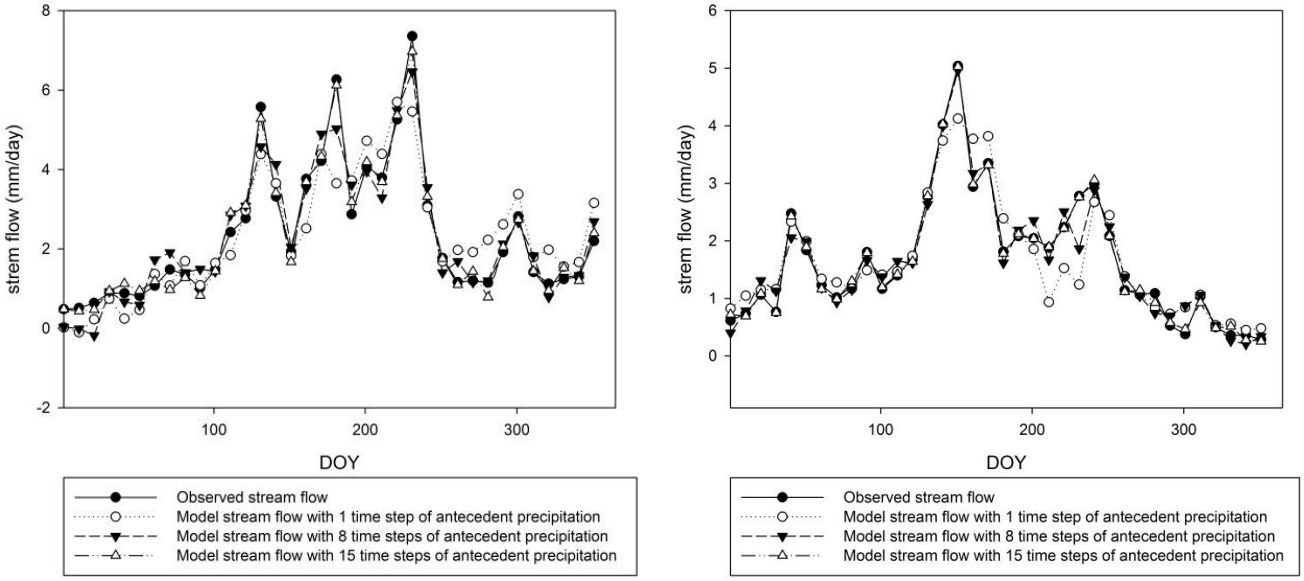

Figure 9: Observed and modelled stream flow using the second implementation of the discrete rainfall-runoff model. The applied durations of antecedent precipitation are 1, 8 and 15 time steps with the time interval of 10 days in 2002 (a) and 2005 (b) respectively .

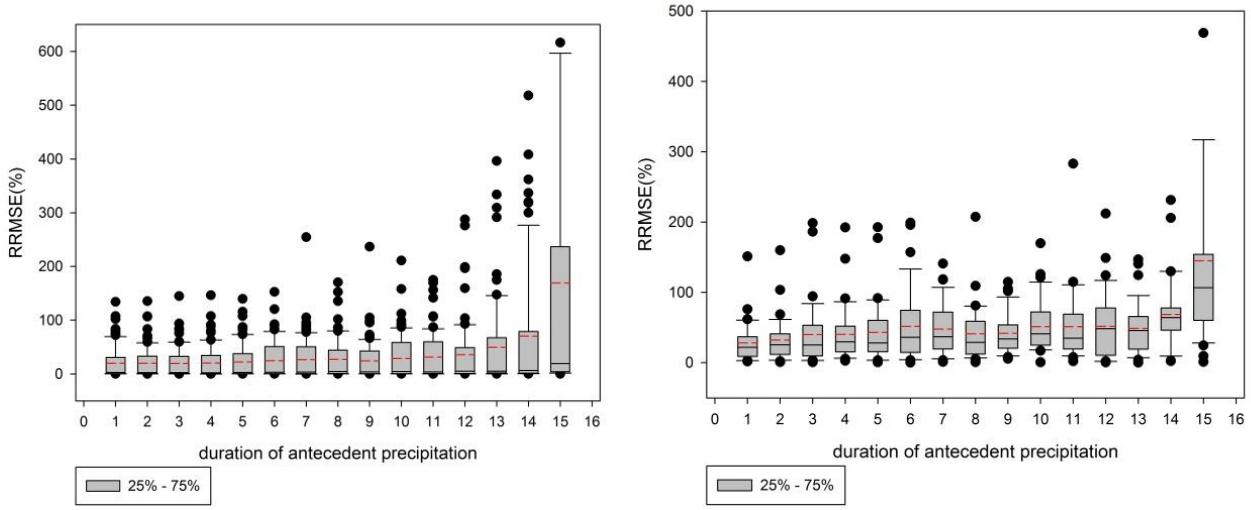

Figure 10: The box plot of the Relative Root Mean Square Error (RRMSE) of the Leave-One-Out cross validation for the second implementation in 2002 (a) and 2005 (b). The duration of antecedent precipitation were increased step-wisely from 1 to 15 time steps with time interval of 10 days. The red dash line in each box is the mean value and the black line is the media value.

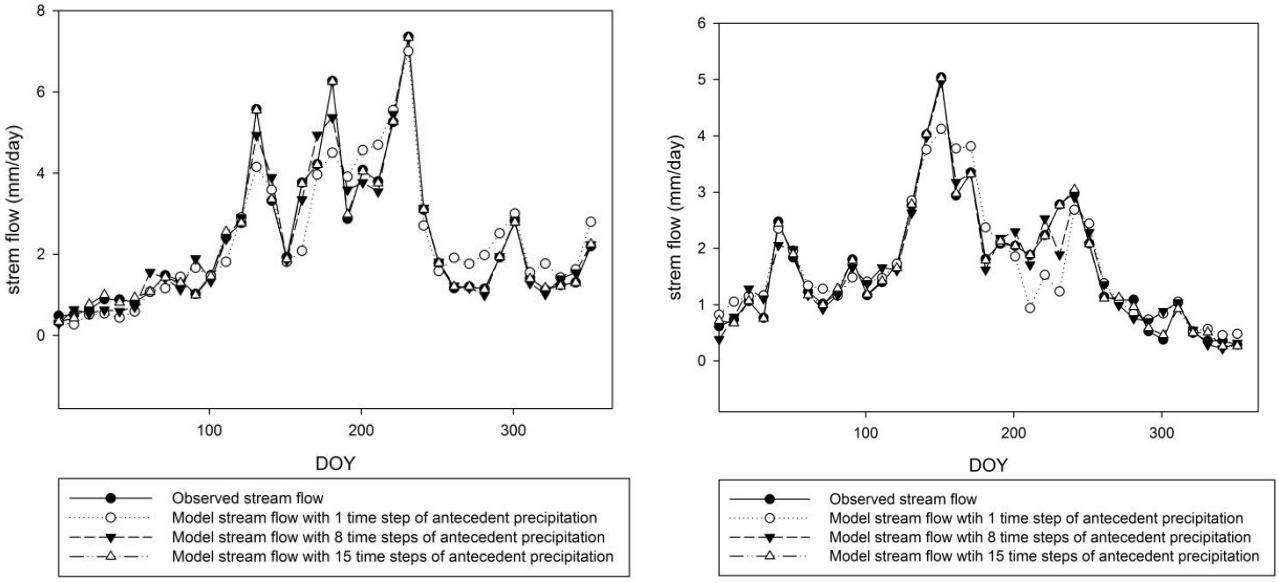

(a) (b)

Figure 11: Observed and modelled stream flow using the third implementation of the discrete rainfall-runoff model. The applied durations of antecedent precipitation are 1, 8 and 15 time steps with the time interval of 10 days in 2002 (a) and 2005 (b) respectively .

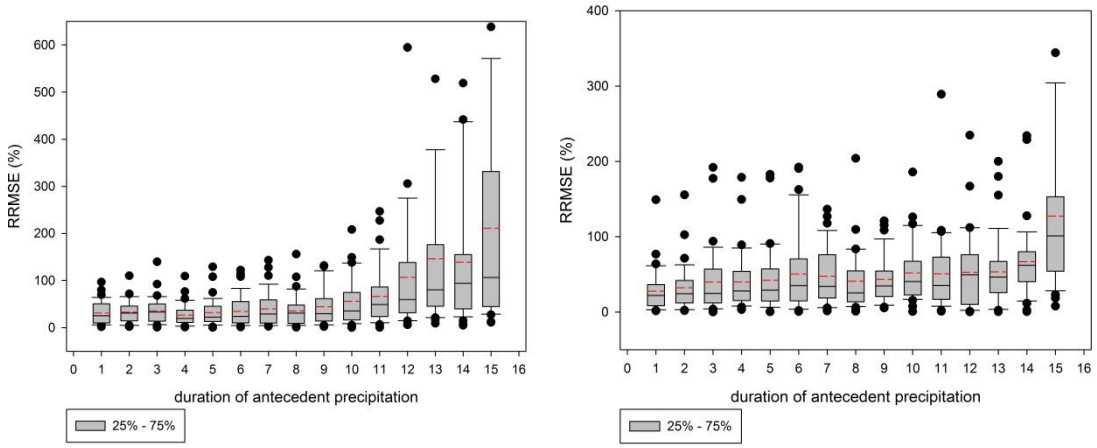

(a) **(b)**

Figure 12: The box plot of the Relative Root Mean Square Error (RRMSE) of the Leave-One-Out cross validation for the second implementation in 2002 (a) and 2005 (b). The duration of antecedent precipitation were increased step-wisely from 1 to 15 time steps with time interval of 10 days. The red dash line in each box is the mean value and the black line is the media value.

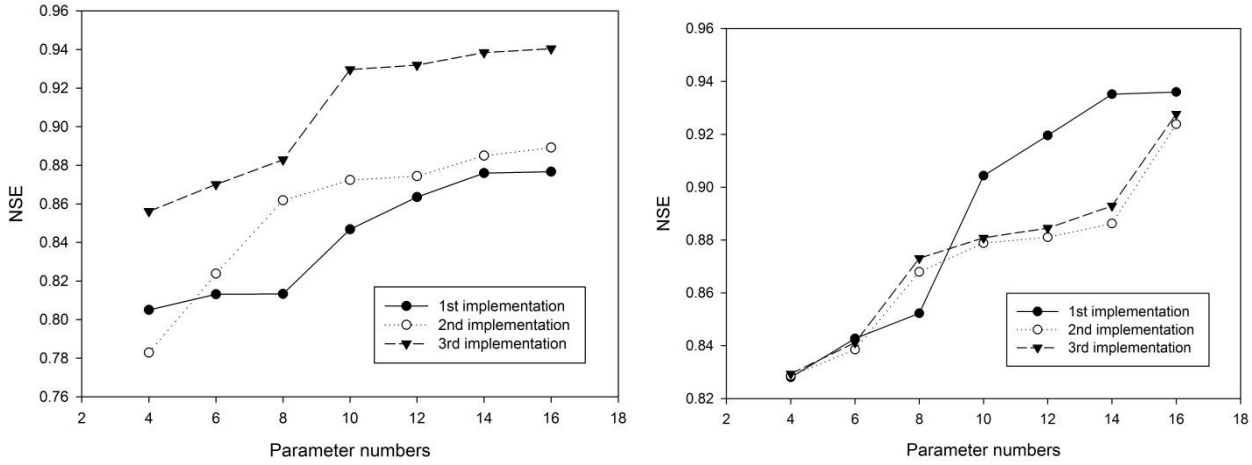

Figure 13: The Nash--Sutcliffe Efficiency (NSE) of three implementations with the same number of model parameters in calibration for 2002 (a) and 2005 (b).

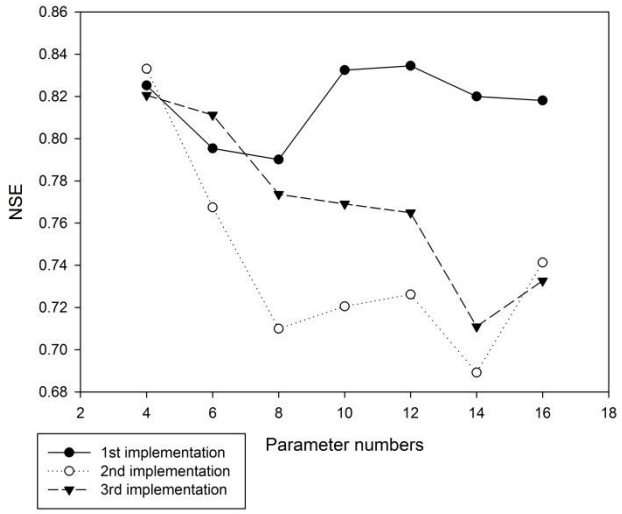

Figure 14: The Nash--Sutcliffe Efficiency (NSE) of three implementations with the same number of averaged model parameters in the validation for 2001.

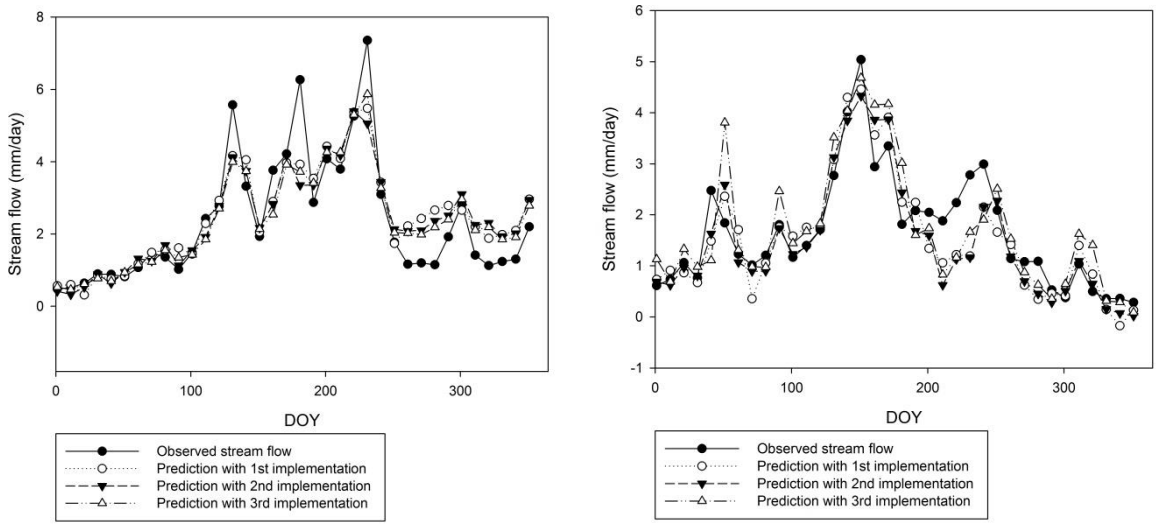

(a) **(b)**

Figure 15: The observed and predicted stream flow in 2002 (a) and 2005 (b) with the three implementations using averaged parameters and the chosen durations.

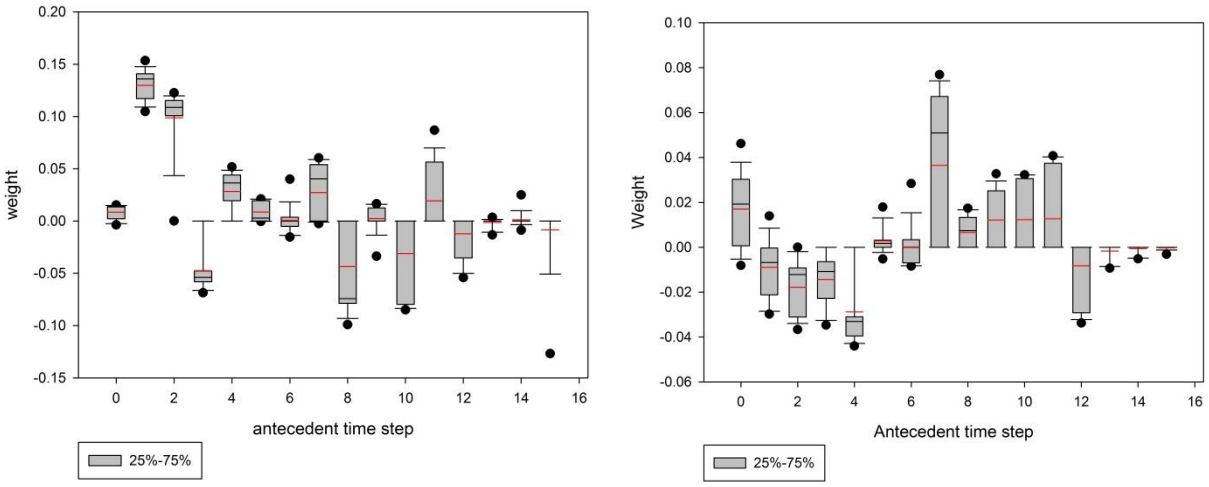

(a) **(b)**

Figure 16: The boxcar plot of precipitation weight at each antecedent time step in calibration of the first implementation. (a) weights in calibration for 2002; (b) weights in calibration for 2005.The duration of antecedent precipitation were increased step-wisely from 1 to 15 time steps in the calibration The red line in box represents the mean values and black line represents the media value.

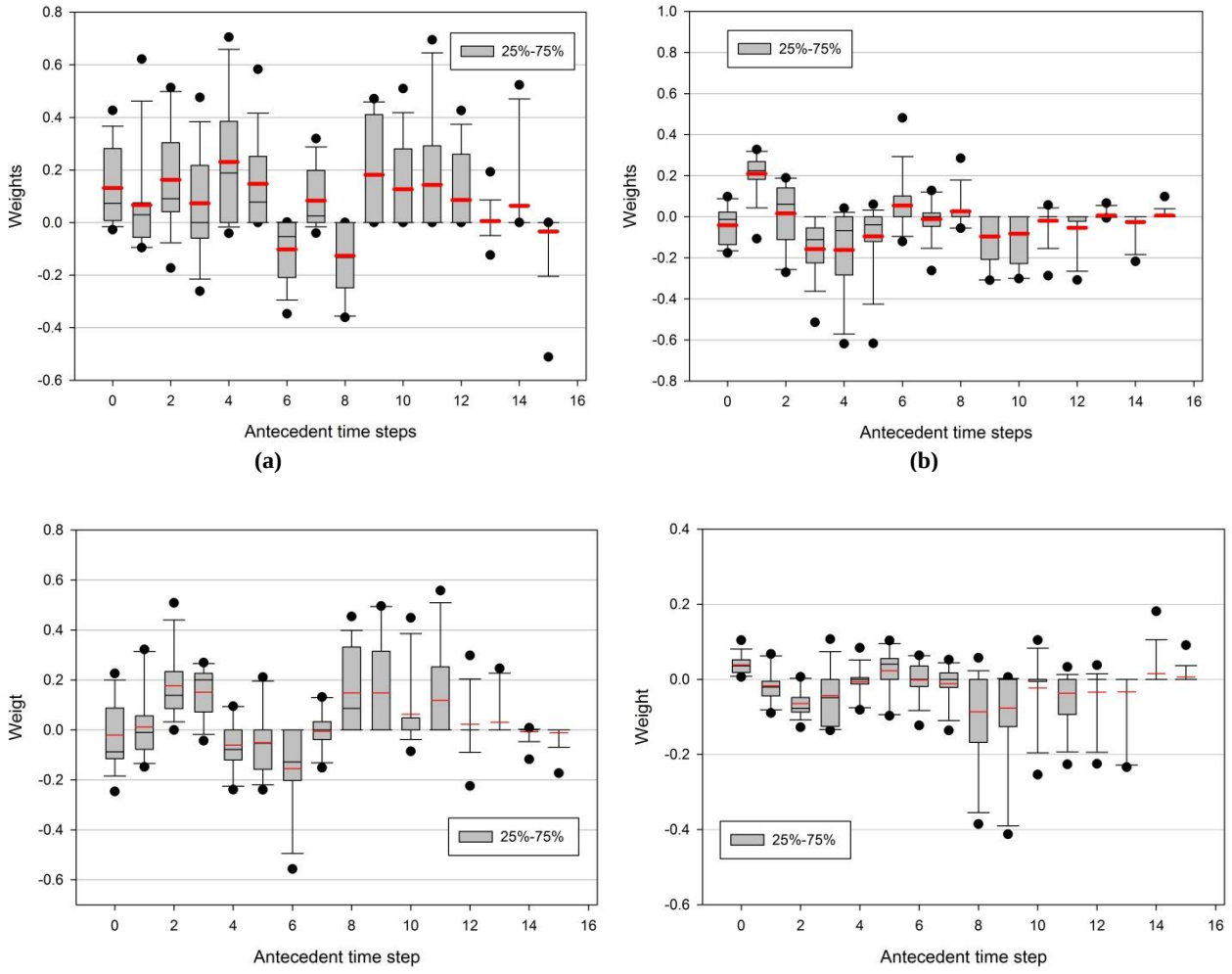

Figure 17: The box plot of weights of overland and infiltrated flow at each antecedent time step in the calibration of the second implementation of the discrete rainfall-runoff model. (a) the weights of overland flow in calibration for 2002; (b) the weights of infiltrated flow in calibration for 2002; (c) the weights of overland flow in calibration for 2005; (d) the weights of infiltrated flow in calibration of 2005. The duration of antecedent precipitation were increased step-wisely from 1 to 15 time steps in the calibration. The red line in box represents the mean values and black line represents the media value.

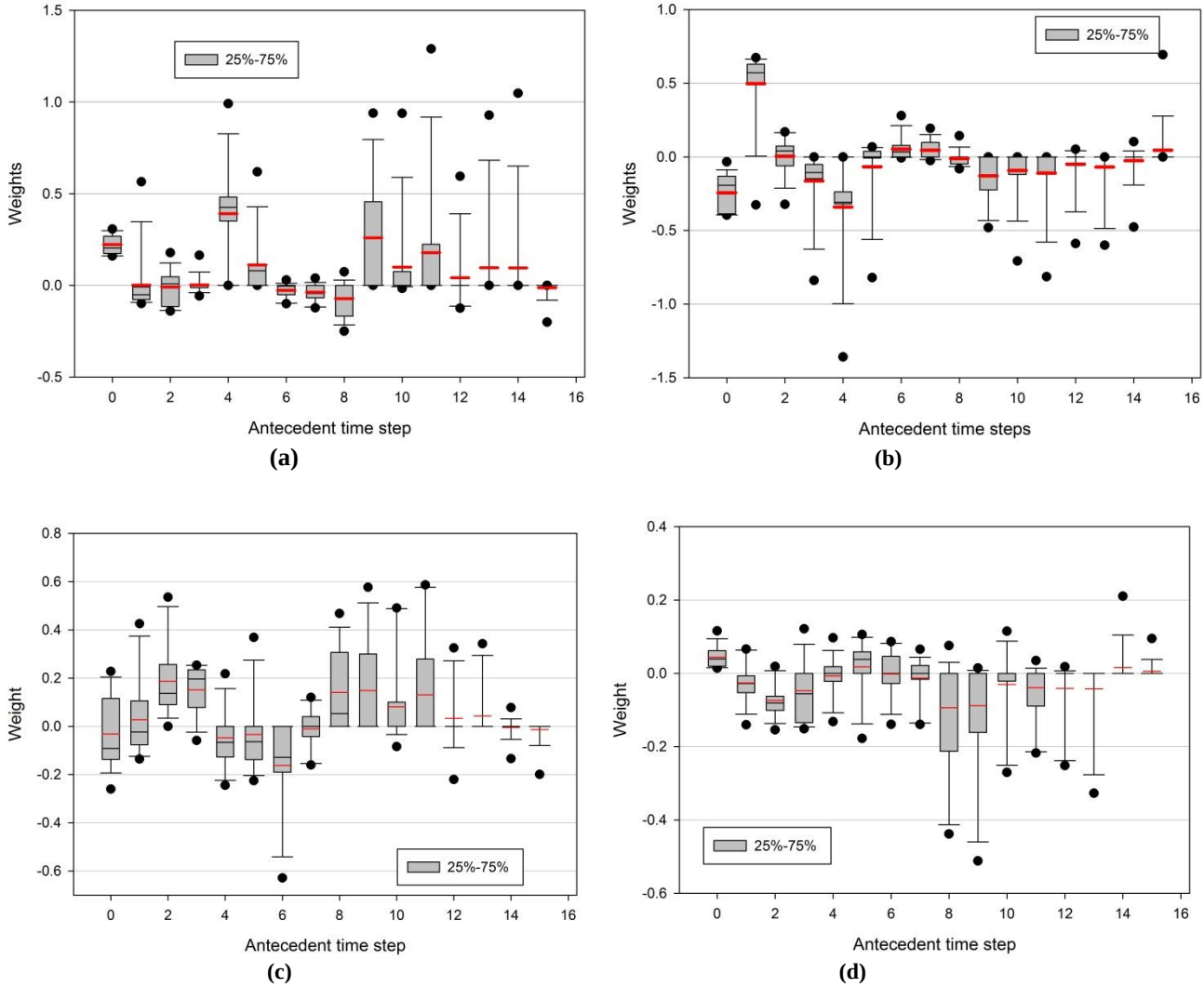

Figure 18: The box plot of weights of overland and potential subsurface flows at each antecedent time step in the calibration of the third implementation of the discrete rainfall-runoff model. (a) the weights of overland flow in calibration for 2002; (b) the weights of potential subsurface flow in calibration for 2002; (c) the weights of overland flow in calibration for 2005; (d) the weights of potential subsurface flow in calibration for 2005. The duration of antecedent precipitation were increased step-wisely from 1 to 15 time steps in the calibration. The red line in box represents the mean values and black line represents the media value.

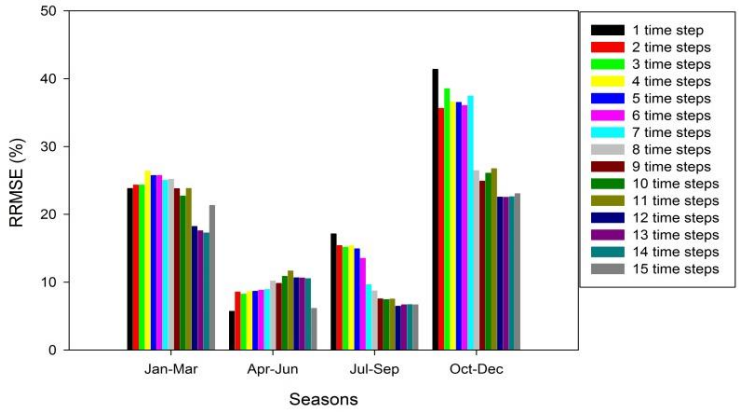

(a)

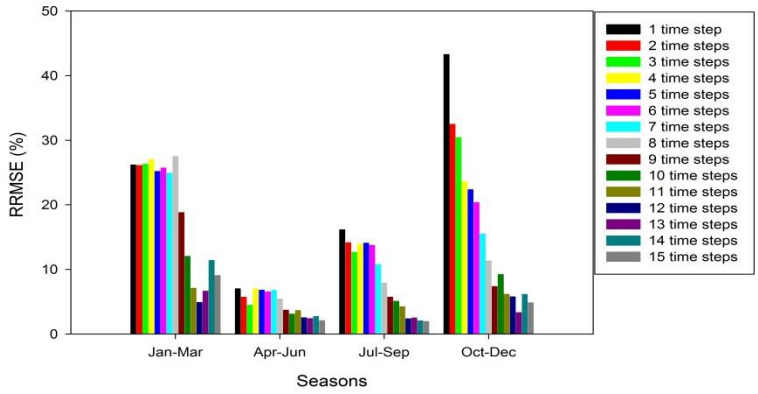

(b)

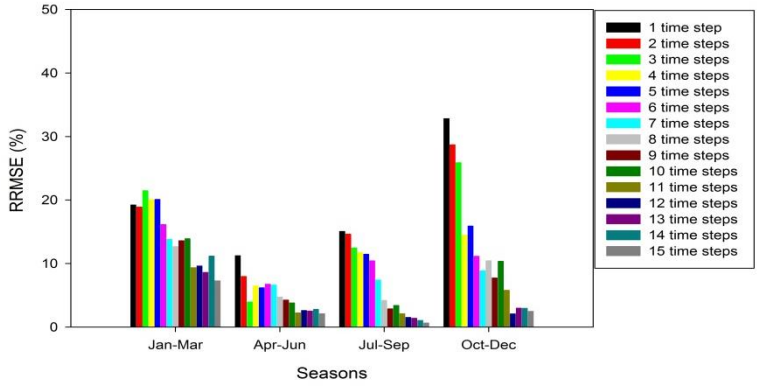

(c)

Figure 19: The Relative Root Mean Square Error (RRMSE) of modelled stream flow in each season during the calibration for both2002 and 2005. (a) the first implementation; (b) the second implementation; (3) the third implementation. The duration of antecedent precipitation were increased step-wisely from 1 to 15 time steps for each implementation